Stony Brook University

Andes Virus Recognition of Human β_3 Integrin is Determined by Residue 33 within the β_3 Integrin PSI Domain

A Dissertation Presented

by

Valery Sofie Matthys

To

The Graduate School

In Partial Fulfillment of the

Requirements

for the Degree of

Doctor of Philosophy

In

Genetics

Stony Brook University

August 2009

Stony Brook University
The Graduate School

Valery Sofie Matthys

We, the dissertation committee for the above candidate for the degree of Doctor of Philosophy, hereby recommend acceptance of this dissertation.

Erich R. Mackow – Dissertation Advisor
Professor – Department of Medicine

Eckard Wimmer – Chairperson of Defense
Professor – Department of Molecular Genetics and Microbiology

Carol Carter
Professor – Department of Molecular Genetics and Microbiology

David Thanassi
Associate Professor – Department of Molecular Genetics and Microbiology

Aniko Paul
Research Associate Professor – Department of Molecular Genetics and Microbiology

This dissertation is accepted by the Graduate School

Lawrence Martin
Dean of the Graduate School

Stony Brook University

Abstract of the Dissertation

Andes Virus Recognition of Human β_3 Integrin is Determined by Residue 33 within the β_3 Integrin PSI Domain

by

Valery Sofie Matthys

Doctor of Philosophy

in

Genetics

Stony Brook University

2009

Andes virus (ANDV) causes a fatal hantavirus pulmonary syndrome (HPS) in humans and Syrian hamsters. Human αvβ3 integrins are receptors for several pathogenic hantaviruses, and the function of αvβ3 integrins on endothelial cells suggests a role for αvβ3 in hantavirus directed vascular permeability. Here we determined that ANDV infection of human endothelial cells or Syrian hamster derived BHK-21 cells was selectively inhibited by vitronectin, a high affinity αvβ3 integrin ligand, and by antibodies to αvβ3 integrins. Further, antibodies to the β3 integrin PSI domain as well

as PSI domain polypeptides derived from human and Syrian hamster β3 subunits, but not murine or bovine β3, inhibited ANDV infection of both BHK-21 and human endothelial cells. These findings suggest that ANDV interacts with β3 subunits through PSI domain residues conserved in both Syrian hamster and human β3 integrins. Sequencing the Syrian hamster β3 integrin PSI domain revealed 8 differences between Syrian hamster and human β3 integrins. Analysis of residues within the PSI domains of human, Syrian hamster, murine and bovine β3 integrins identified unique proline substitutions at residues 32-33 of murine and bovine PSI domains that could determine ANDV recognition. Mutagenizing the human β3 PSI domain to contain the L33P substitution present in bovine β3 integrin abolished the ability of the PSI domain to inhibit ANDV infectivity. Conversely, mutagenizing either the bovine PSI domain, P33L, or the murine PSI domain, S32P, to the residue present human β3 permitted PSI mutants to inhibit ANDV infection. Similarly, CHO cells transfected with the full length bovine β3 integrin containing the P33L mutation, permitted infection by ANDV. These findings indicate that human and Syrian hamster αvβ3 integrins are key receptors for ANDV and that specific residues within the β3 integrin PSI domain are required for ANDV infection. Since L33P is a naturally occuring human β3 polymorphism these findings further suggest the importance of specific β_3 integrin residues in hantavirus infection. These findings also rationalize determining the role of β3 integrins in hantavirus pathogenesis in the Syrian hamster model.

Table of Contents

List of Tables

List of Figures

CHAPTER 1:

Introduction

Section I: Hantaviruses

Historical Perspective

During the Korean war, over 3,000 UN soldiers suffered from a previously unknown disease. Soldiers presented an acute febrile disease with hemorrhagic symptoms and renal complications and the mortality rate was 5-10% (15, 60). It was not until 1973 that the causative agent for this Korean Hemorrhagic Fever (KHF) was identified (60). Scientists isolated the virus from its natural host, *Apodemus agragius* or the striped field mouse, and named it Hantaan virus after the Hantaan river in Korea (60, 95). It became clear that Hantaan virus was responsible for outbreaks of so called "trench" nephritis amongst Japanese troops in 1913 and a similar disease had also plagued German and Allied troops during World War I (60, 61).

After isolation of Hantaan virus, other forms of the virus were discovered throughout Asia (Seoul), Eastern Europe (Dobrava, Puumala), and Scandinavia (Puumala) (15, 61, 66, 95), and these viruses were classified as Hantaviruses. Hantaviruses in Asia and Europe cause what is now called Hemorrhagic Fever with Renal Syndrome (HFRS), with Hantaan and Dobrava virus resulting in severe HFRS and the Puumala virus leading to a disease with less mortality (15, 47) (Table 1).

In 1993, over one hundred people from the four corners region in the Southwestern United States suffered from an unexplained pulmonary illness and about 50% of the cases resulted in death (47, 76, 80, 131). Patients suffered flu-like symptoms for a few days followed by acute pulmonary edema and severe

thrombocytopenia (76, 80). Their condition deteriorated rapidly and patients died within a few hours of respiratory distress onset.

Serum taken from patients showed an antibody response against the hantavirus antigen and the agent was identified as a previously unknown hantavirus (76, 80, 95, 131). The hantavirus isolated was later named Sin Nombre virus (SNV) (80, 95), and caused a clinically distinct disease in comparison to those infected with Eurasian hantaviruses. SNV infected patients developed an acute pulmonary component and the disease was termed Hantavirus Pulmonary Syndrome (HPS). After the discovery of SNV, ~25 other hantaviruses causing HPS were identified in North America (47, 74, 76, 94, 95). Another 15 HPS causing hantaviruses have also been identified in Southern and Central America (47, 80, 131) (Table 1). The incidence of HPS is much lower than that of HFRS in Asia and Europe, as only about 1000 HPS cases in the US have been documented since 1993. However, even with treatment, the mortality rate of HPS remains high, 35-40% (76, 80).

Although hantaviruses are predominantly pathogenic, two notable non-pathogenic hantaviruses, Prospect Hill virus (PHV) in America carried by meadow voles (*Microtus pennsylvanicus*) and TULA virus (TULA) carried by the common vole (*Microtus arvalis*), are not associated with any human disease (94, 95) (Table 1).

Hantavirus hosts and transmission

Hantaviruses form a unique genus within the Bunyviridae family, along with Orthobunyavirues, Nairoviruses, Phleboviruses and Tospoviruses (95). Hantaviruses

are the only members of the Bunyaviridae, which are not arthropod borne (84, 94). Hantaviruses in Europe and Asia (Old World hantaviruses) are carried by Murinae rodents (Old World Rats and Mice) and Arvicolinae (voles, lemmings and muskrats (95), while hantavirus in the Americas (New World hantaviruses) are carried by Sigmodontinae (New World Rats and Mice) (40, 84, 95).

Hantaviruses persistently infect their natural hosts and each hantavirus has co-evolved with a primary host (84). Therefore, the relationship between hantaviruses and their hosts coincides with their genetic evolution and defines the geographic prevalence of hantaviruses and hantavirus disease (84, 95).

The hosts are persistently infected with hantaviruses but are asymptomatic (84, 95). It is not known how hantaviruses evade host immune responses or why the virus is nonpathogenic in its animal hosts. Hosts secrete virus for prolonged periods of time and host to host transmission occurs through excreted virus as well as biting, indicating that hantavirus can be spread through saliva (47, 84, 94). Hantavirus transmission to humans occurs through the inhalation of aerosolized viral particles excreted by rodents in their urine and feces (47, 84). In general, hantavirus transmission between humans does not occur, although there are several reported cases in which the South-America Andes hantavirus (ANDV) was spread person to person between members of the same household and physicians (21, 79, 113, 126) .

Hantavirus Disease

Pulmonary endothelial cells are primary sites of infection in both HFRS and HPS patients (15, 94, 131). However, the endothelium of all organs, including the heart, kidney, liver, and spleen is also infected. Hantavirus disease is characterized by increased vascular permeability, acute thrombocytopenia, hemorrhage, and pulmonary edema without endothelial lysis. In HFRS, the most damage is seen in the kidneys, whereas in HPS, the lungs and the spleen are mostly affected (94, 95).

Clinical features of HFRS

The incubation time is generally 1-2 weeks post exposure and the initial symptoms of HFRS are non-descript and include high fever, myalgia, chills, headache, and abdominal and back pain (15, 81, 94, 95). Patients may also present with proteinuria, an indication of renal failure. After 4-6 days, the disease progresses to a hypotensive stage, where patients suffer from tachycardia and thrombocytopenia (17, 81) which lasts from hours to days. The main characteristics of the subsequent oliguric stage are oliguria, bleeding tendency, and edema (17, 81, 95). A diuretic stage follows in which patients suffer from rapid dehydration, which leads to severe shock if fluid intake is inadequate. This stage can last two to three weeks, after which patients enter the convalescent stage, which may last up to one year (81, 95). Not every patient will present all of these stages and this can make the diagnosis of HFRS difficult. The severity of disease is determined by the infecting hantavirus and therefore the geographical distribution of the virus and its host (84). The most severe types of HFRS are Korean Hemorrhagic Fever caused by Hantaan virus transmitted

by the striped field mouse (*A. agrarius*), and Balkan Hemorrhagic fever caused by Dobrava virus and transmitted by the yellow-necked field mouse (*A. flavicollis*) (84, 95). Puumala virus is transmitted by the European bank vole (*Clethrionomys glariolus)* and leads to a mild form of HFRS (also called nephropathia endemica) (84, 95). HFRS has a mortality rate ranging from 0.1-5%, with causes of death including shock (75%), uremia (50%), pulmonary edema (15%), and central nervous system hemorrhage or encephalopathy (5%). Full recovery from HFRS often takes from 6 months to a year (17, 95).

Clinical features of HPS

Similar to HFRS, symptoms of HPS begin 2-3 weeks post hantavirus infection. Patients initially suffer from flu-like symptoms and after 4-10 days develop pulmonary edema and acute thrombocytopenia (76, 80, 81, 94, 95, 131). Subsequently the patient's condition rapidly deteriorates and hospitalization is needed. HPS is characterized in four stages (febrile, cardiopulmonary, diuretic, and convalescent) and has a mortality rate of approximately 40%, with pulmonary edema and cardiovascular shock being the main causes of death (76, 80, 81, 94, 95, 131).

Similarities and differences between HFRS and HPS

HFRS and HPS causing hantaviruses infect the pulmonary endothelial cells of hosts and humans. Both diseases feature initial flu-like symptoms and either disease can manifest renal and pulmonary components (76, 81). Common characteristics of HFRS and HPS include vascular permeability, hemorrhage or edema and thrombocytopenia (17, 76, 81, 131). However, it is unclear what triggers vascular

permeability in hantavirus disease or why Eurasian hantaviruses cause hemorrhagic disease while American hantaviruses cause edema with little or no hemorrhage sequalae (17, 76, 131). These observations suggest that there are common elements to hantavirus disease that affect vascular permeability but also indicate a fundamental difference in the mechanism of HFRS and HPS diseases (81, 95).

Treatment

For both HFRS and HPS, treatment consists largely of supportive care including fluid management, controlled electrolyte balance, and ventilation support (69). In some HFRS cases, the anti-viral drug Ribavirin has been shown to be an effective form of treatment, but only when administered early after infection. Ribavirin does not seem to be effective for treatment of HPS (69). Interferon can be an effective treatment for HFRS and HPS but only when administered far before the onset of symptoms, which means that few patients benefit from it as a therapeutic agent (47, 69).

Hantavirus structure

Like other Bunyaviruses, hantaviruses are enveloped negative-stranded RNA viruses (85, 95) (Figure 1). Hantavirus particles average 100 nm in diameter with a spherical shape and a highly structured, grid-like pattern on their surface formed by the viral surface glycoproteins (85, 94, 95). The hantavirus genome consist of three segments: Small (S) segment, the Medium (M) segment and Large (L) segment (94, 95). Each segment has conserved and complementary nucleotides on their 5' and 3'

ends that are capable of forming panhandle structures (85, 100). The high degree conservancy between these untranslated regions (UTRs) in hantaviruses and Bunyaviruses are believed to play an important role in viral replication and transcription (48, 100). Nucleotide sequence comparison among discrete hantavirus serotypes shows a 60-70% identity among all three RNA segments (85, 94).

The S segment encodes the nucleocapsid protein or N protein. The N protein is the most abundantly expressed hantavirus protein and is also the major antigenic determinant of the virus. The N protein is expressed at high levels in infected cells and is detectable 6 hours after infection (85). The nucleocapsid protein can form dimers and trimers and encapsidates the viral genomic RNA and cRNA. It is likely that the N protein participates in viral replication, protects viral RNA from cellular degradation and plays a role in virion assembly (47, 85).

The M segment encodes a glycoprotein precursor. The glycoprotein precursor is co-translationally cleaved into two glycoproteins, Gn (N-terminal glycoprotein) and Gc (C-terminal) glycoprotein, presumably by cellular signal peptidases present in the ER (47, 85, 98). For all hantaviruses, cleavage occurs after the conserved WAASA amino acid motif (64, 85). Gn and Gc glycoproteins are type I integral transmembrane proteins with the N-terminus located in the lumen of the ER and the C-terminus in the cytoplasm (47, 98). Gn contains a predicted signal sequence, several transmembrane domains, a double hydrophobic anchor sequence, predicted RING and zinc-finger domains, and a 142 amino acid long cytoplasmic tail that contains an ITAM motif

(30, 31). The cytoplasmic tail of Gc is very short, only 9 amino acids long, and contains a putative ER retention signal (85).

Co-expression of hantavirus glycoproteins results in trafficking both glycoproteins to the ER and cis Golgi, where glycosylation is completed (48, 64, 95, 98). Expression of either glycoprotein individually results in Gn appearing to localize to the cis-Golgi while Gc is retained in the ER (64, 94, 98). The domains responsible for retention in the ER and trafficking to the Golgi were identified in the cytoplasmic domains and transmembrane domains of both glycoproteins (48, 64, 98). The trafficking and retention within the cis-Golgi is required for the maturation of virions and is a hallmark for all members of the Bunyaviridae (48, 78, 94, 98, 100). Mature virions bud into the lumen of the Golgi and apparently exit the cell through secretory vesicles (100).

The L segment encodes the 220 kDa RNA dependent RNA polymerase (RdRp) and is highly conserved among hantaviruses (47). After viral entry, there is a short primary transcription by the RdRp. This primary transcription produces more templates for mRNA and genomes for viral progeny (47, 100). An unknown signal then initiates viral replication which requires primers derived from host mRNAs (100). The viral polymerase is involved in a process called cap snatching although it is unclear where this process occurs and recent studies indicate that this could occur within cytoplasmic P-bodies (71). The RdRp presumably acts as an endonuclease to cleave the 5' cap of host mRNAs and generate primers necessary for viral mRNA transcription (47, 100).

Hantavirus regulation of Interferon Responses

Non-pathogenic PHV elicits early interferon (INF) responses in humans, suggesting that hantavirus pathogenesis may in part be determined by viral regulation of cellular interferon responses. In contrast to pathogenic NY-1V and HTNV, PHV replication is blocked in IFN competent human endothelial cells, further suggesting NY-1V and HTNV might regulate early IFN responses (2, 32). Further findings have shown that the NY-1V Gn cytoplasmic tail inhibits RIG-I and TBK1 directed transcription from interferon stimulated response elements (ISRE) or β-interferon promoters (2). In contrast, expression of the NY-1V nucleocapsid protein or PHV Gn-tail had no effect on RIG-I or TBK1 directed transcription (2). Further, neither the NY-1V nor PHV Gn-tails inhibited transcriptional responses directed by a constitutively active IRF-3 protein. These findings indicate that the pathogenic NY-1V Gn protein regulates cellular IFN responses upstream of IRF-3 phosphorylation at the level of TBK1 signaling complexes (2).

TBK1 phosphorylates IRF-3, and forms a signaling complex with TRAF3, which is required for IFN transcription directed by a variety of upstream stimuli. Studies have shown that the NY-1V Gn-tail co-immunoprecipitates TRAF3, but not TBK1, from cellular lysates (2, 3). Analysis of TRAF3 deletion mutants demonstrated that the Gn-tail bound the N-terminus of TRAF3. In contrast, the Gn-tail of the non-pathogenic hantavirus PHV failed to bind TRAF3 proteins or inhibit IFN-β transcriptional responses. Expression of NY-1V blocked TBK1 co-precipitation of TRAF3 and, similarly, infection by NY-1V, but not PHV, blocked the formation of

TBK1-TRAF3 complexes (2, 3). These findings suggest that both the NY-1V Gn-tail and infection by NY-1V virus disrupt the formation of TBK1-TRAF3 signaling complexes required for IFN-β induction (2, 3).

These findings indicate that the ability to inhibit interferon-β induction at early times post-infection is critical for hantavirus infection of human endothelial cells and suggest that the pathogenic hantavirus Gn cytoplasmic tail is the primary determinant of hantavirus pathogenic potential in humans (2, 3, 32).

The Hantavirus Gn Cytoplasmic Tail is Degraded by the Proteosome

The Gn cytoplasmic tail of pathogenic hantaviruses contains a degradation motif or degron at its C-terminus (30, 96). In contrast, the Gn cytoplasmic tail of the non-pathogenic hantavirus PHV is stable and reciprocal changes between NY-1V and PHV identified 4 residues in NY-1V that determine stability (96). Analysis of the differences between PHV and NY-1V domains identified a hydrophilic moment within a largely hydrophobic domain that was required for proteosomal degradation (96). This also suggests that stability differences between the Gn tails of pathogenic and non-pathogneic hantaviruses may differentially regulate cell signaling responses that contribute to viral pathogenesis (96).

Syrian Hamster Model for Hantavirus Disease

The absence of an animal model of HPS and HFRS has made studying hantavirus pathogenesis difficult. Although hantavirus hosts are referred to as “mice”,

these small mammals are discrete species that are more similar to voles and hamsters (8, 85) and in fact, *Mus musculus* is not a hantavirus host. *Rattus rattus* and *Rattus norvegicus* are hosts for Seoul virus but since they do not develop disease, they are also unsuitable as animal models (85). In 2001, reports showed that Syrian hamsters infected with Andes virus (ANDV) develop a disease that is similar to human HPS (43, 44). The onset of ANDV disease in Syrian hamsters is 10-14 days and occurs rapidly with ANDV replication primarily in endothelial cells of pulmonary capillary beds (44, 121). Six days post-infection ANDV is present in the blood (viremia) and focal pulmonary edema can already be detected. Endothelial cell inclusions become visible and Syrian hamsters show increased white blood cell counts and lymphopenia. Twelve to 14 days post-infection, Syrian hamsters develop severe pulmonary edema with a 90% mortality rate (44, 121).

Interestingly, within two days post-infection ANDV viremia reached 10^7 PFU/ml while Syrian hamsters infected with the prototypic HPS causing Sin Nombre virus (SNV) never developed viremia (121). Even 12 days after infection little SNV antigen was detected in Syrian hamster endothelial cells (121). ANDV and SNV are closely related serotypes but it is unknown why ANDV is lethal in Syrian hamsters while SNV fails to replicate (43, 121). Syrian hamsters are currently the only animal model of hantavirus pathogenesis and serve as an important tool for studying hantavirus pathogenesis and for development of antiviral drugs for hantavirus disease (43) .

Hantavirus Receptors

Both pathogenic and non-pathogenic hantaviruses predominantly replicate in endothelial cells but cause little or no damage to the endothelium and virus can be passaged with infected endothelial cells (69, 81). Only pathogenic hantaviruses cause vascular permeability, however; nonpathogenic hantaviruses enter human endothelial cells demonstrating that viral entry alone is not the only determinant of hantavirus disease (68, 81, 94). However, the means by which pathogenic hantaviruses cause pulmonary edema and hemorrhage has yet to be defined. Pathogenic hantaviruses bind human β_3 integrin subunits present within $\alpha_v\beta_3$ and $\alpha_{IIb}\beta_3$ integrins. These heterodimeric receptors are abundantly expressed on the cell surface of endothelial cells and platelets (26, 29, 68). $\alpha_v\beta_3$ integrins on endothelial cells are regulators of vascular barrier function, maintain capillary integrity, play a role in immune cell recruitment and direct cell migration and angiogenesis (12). Initial experiments showed that pathogenic hantavirus infection is inhibited by vitronectin, a high affinity ligand for $\alpha_v\beta_3$ integrin and by antibodies against $\alpha_v\beta_3$ integrins (26, 29, 68). Antibodies to the β_3 integrin subunit selectively inhibited infection by pathogenic hantaviruses demonstrating that only pathogenic hantaviruses recognize β_3 integrins (26, 29, 68). Expression of $\alpha_v\beta_3$ integrin on the surface of non-susceptible cells such as CHO cells confer infection to pathogenic hantavirus and this infection is inhibited by antibodies to $\alpha_v\beta_3$ or the β_3 integrin subunit (26, 68). In contrast, the non-pathogenic hantavirus PHV is inhibited by fibronectin, a high affinity ligand for $\alpha_5\beta_1$ integrin and by antibodies against $\alpha_5\beta_1$ integrin (26, 29, 68). These experiments

indicate that $\alpha_v\beta_3$ integrins not only determine pathogenic hantavirus entry but may also play a key role in hantavirus pathogenesis.

Integrin ligands like vitronectin, contain an arginine-glycine-aspartic acid (RGD) recognition sequence which partially mediates ligand binding to $\alpha_v\beta_3$ integrins (33). Hantavirus surface glycoproteins Gn and Gc do not contain RGD motifs suggesting that hantavirus binding to $\alpha_v\beta_3$ integrins is not directed by RGD recognition sequences. This was demonstrated through experiments showing that hantavirus infection is not inhibited by RGD peptides and that hantaviruses could enter CHO cells expressing mutant $\alpha_{IIb}\beta_3$ integrins incapable of binding the RGD recognition sequence (26, 68). These results suggested that hantavirus binding to β3 integrins occurs through unique interactions.

Even though $\alpha_v\beta_3$ integrins are highly conserved among different species, the human β_3 subunit serves as a receptor for pathogenic hantaviruses while murine and bovine β_3 integrin subunits were not recognized by hantaviruses (86). This permitted the use of domain swaps for the identification of β_3 integrin domains required for hantavirus recognition (86). A recombinant murine β_3 integrin containing the N-terminal 43 amino acids of human β_3 was found to confer hantavirus infectivity when expressed on the surface of CHO cells (86).

The N-terminal domain of β_3 integrin is also called the Plexin-Semaphorin-Integrin (PSI) domain and polypeptides expressing the human β_3 integrin PSI domain were also found to inhibit pathogenic hantavirus infection (86). In contrast, the murine β_3 integrin PSI domain was incapable of inhibiting hantavirus infection. These

findings demonstrated that specific β_3 integrin residues, which differ between human and murine PSI domains, determine hantavirus recognition (86). Raymond et al. (86) reported that the aspartic acid residue at position 39 (D39) in human β_3 integrin was required for β_3 integrin recognition by pathogenic hantaviruses NY-1V and HTNV. When D39 in the full length human β_3 integrin was changed into its murine homologue, aparagine (N39), the mutant integrin failed to confer cell susceptibility to NY-1 and HTNV. Similarly, polypeptides expressing the human PSI domain with a D39N change, failed to inhibit NY-1V and HTNV infectivity (86).

Integrins exist in two conformations, an active extended conformation and a bent, inactive conformation (Figure 2). In the active conformation, the RGD ligand binding domain of the $\alpha_v\beta_3$ integrin is located at the apex of the extended integrin while in the inactive integrin conformation, the ligand binding domain is folded towards the cell membrane rendering it inaccessible for ligand binding (105, 130). Interestingly, the bent $\alpha_v\beta_3$ integrin conformation places the PSI domain at the apex of the inactive integrin (130). This suggested that the PSI domain, hidden in the active integrin conformation, is accessible for hantaviruses when the integrin is in the inactive conformation.

The $\alpha_v\beta_3$ integrin conformation is influenced by selected divalent cations. Studies have shown that ligand binding to the $\alpha_v\beta_3$ integrin is enhanced in the presence of magnesium and manganese which puts the $\alpha_v\beta_3$ integrin in an active state. However, RGD ligand binding is reduced in the presence of calcium, which puts $\alpha_v\beta_3$ integrin into its bent conformation (105, 130). This understanding explains results

demonstrating that hantavirus infection is inhibited by manganese pretreatment and enhanced by calcium (86). These findings are also consistent with structural changes within the $\alpha_v\beta_3$ integrin that determine hantavirus interactions with β_3 integrins. These results were confirmed by experiments using locked bent $\alpha_v\beta_3$ integrin conformer, which enhanced hantavirus infectivity compared to cells expressing a locked extended $\alpha_v\beta_3$ conformer (86). Thus, locking $\alpha_v\beta_3$ in its bent conformation confers hantavirus infectivity and rationalizes hantavirus binding to the β3 PSI domain (86). This data also indicates that pathogenic hantavirus interactions with bent αvβ3 integrins may block $\alpha_v\beta_3$ integrin functions by keeping the integrin in an inactive bent state.

Pathogenic Hantaviruses Enhance Endothelial Cell Permeability in Response to VEGF

$\alpha_v\beta_3$ integrins direct endothelial cell migration necessary for angiogenesis, wound repair and vascular permeability through interaction with the vascular endothelial growth factor receptor 2 (VEGFR2) (11, 42, 87, 89). VEGF, the ligand for VEGFR2, directs migration on vitronectin and VEGF was originally named vascular permeability factor (VPF) for its ability to enhance permeability and cause edema (11, 89). Because pathogenic hantaviruses bind inactive $\alpha_v\beta_3$ conformers, the effect of hantavirus infection on endothelial cell migration as well as the permeability of infected endothelial cells was evaluated (27, 28, 86). Gavrilovskaya et al. (28) showed that endothelial cell migration on the high affinity β_3 integrin ligand, vitronectin, was blocked by pathogenic hantaviruses and this effect was similar to migration blocked

by antibodies directed against β_3 integrins. Endothelial cell migration was inhibited as early as 24 – 48 hours post infection. In contrast, non-pathogenic hantaviruses did not block endothelial cell migration on either β_3 or β_1 integrins (28).

A recent report has also shown that pathogenic NY-1V, ANDV and HTNV hantaviruses enhance the permeabilizing responses of endothelial cells in response to VEGF with the most dramatic effect observed at late times post infection (3 days) (27). Pathogenic hantaviruses alone are not able to permeabilize endothelial cells and non-pathogenic hantaviruses PHV and TULA failed to alter the permeability of infected endothelial cells in the presence or absence of VEGF (27). Pretreatment of endothelial cells with an antibody against VEGFR2 reduced the permeabilizing effects of pathogenic hantaviruses in presence of VEGF by 50 – 75% demonstrating that hantavirus-directed endothelial cell permeability is dependent on the function of VEGFR2 (27). These findings show that pathogenic hantaviruses interact with αvβ3 integrins which normally regulate endothelial cell responses to VEGF.

VEGF directed permeability is further impacted by endogenous and exogenous cellular factors including angiopoietin 1 and sphingosine-1-phosphate (S1P), which regulate endothelial cell permeability through effects on cellular VEGF responses (9, 27). Angiopoietin1 (Ang1) is another endothelial cell specific growth factor, however Ang-1 counters the permeabilizing effects of VEGF and stabilizes the vasculature (111, 112). Ang1 binds to Tie-2 receptors and has a dominant effect over the permeabilizing responses of co-administered VEGF in vitro and in vivo (111, 112). Ang-1 stabilizes capillaries, directs the assembly of adherens junctions and

promotes vascular barrier functions (111, 112). Aside from the role of platelets in clotting cascades, platelets also contribute to endothelial cell barrier function by releasing the lipid mediator S1P, which regulates endothelial cell permeability (93, 107). Activated platelets release S1P which binds to G-protein coupled Edg-1 receptors on endothelial cells. S1P enhances the accumulation of vascular-endothelial cadherin (VE-cadherin), present in endothelial cell adherens junctions (93, 107). Interestingly, addition of both Ang1 and S1P addition to hantavirus infected cells blocked the heightened permeability of endothelial cell monolayers in response to VEGF suggesting that they are of potential therapeutic importance for hantavirus disease (9, 27).

The Role of the Endothelium in Viral Hemorrhagic Fevers

Hantaviruses mainly replicate within endothelial cells. The endothelium forms a multifunctional barrier that lines every blood vessel and comes in contact with many pathogens. The endothelium plays a role in the disease process either by functioning as a direct target of the pathogen or through its involvement in the inflammatory response (14, 39, 116). The endothelium performs a primary fluid barrier function and ultimately contributes to all viral hemorrhagic diseases. Although not all viral hemorrhagic fevers target endothelial cells specifically, viral hemorrhagic fevers are hallmarked by endothelial dysfunction with increased vascular permeability or vascular damage and the role of endothelial cells and platelets in many of these diseases has yet to be analyzed. In nearly all viral hemorrhagic disease permeability

occurs concomitantly with thrombocytopenia and severely depressed platelet functions (82).

Bunyaviruses

Hantaviruses: All hantaviruses have the ability to enter endothelial cells regardless of whether they cause HFRS, HPS or are non-pathogenic. However, not all hantaviruses replicate successfully in endothelial cells. As described above, the non-pathogenic hantavirus PHV cannot circumvent early interferon responses and fails to replicate within human endothelial cells (2, 32). This indicates that at one level hantavirus pathogenesis is determined by the viruses ability to regulate innate cellular responses which inhibit replication (3). A second means for pathogenic hantaviruses to cause disease may stem from the accidental dysregulation of normal endothelial functions that dynamically alter endothelial cell barrier functions.

Rift Valley Fever and Crimean Congo Hemorrhagic Fever: Late interferon-α responses allow Rift Valley Fever infection of the vascular endothelium and determines the severity of Rift Valley Fever. The viral infection itself destroys the vascular lining of the capillaries glomeruli and causes severe damage to the endothelium (82). Crimean Congo Hemorrhagic Fever (CCHF) virus leads to severe hemorrhage but is not highly cytopathic. It is not clear whether vascular permeability in CCHF is caused by damage to the endothelial cells or by disruption of the endothelial cell junctions which normally form a fluid barrier (82, 125).

Filoviruses:

Ebola and Marburg viruses are very invasive, cytopathic viruses which primarily infect monocytes, macrophages and dendritic cells but rapidly spread to the endothelium of many organs (1, 82). Infected macrophages release high amounts of pro-inflammatory cytokines, which target the vascular system in particular and lead to disruption of endothelial adhesions. In addition, direct infection of the endothelium leads to reorganization of adherence and junction proteins and contributes to increased permeability and loss of vascular integrity (1, 82).

Arenaviruses

Examples of Arenaviruses are Lassa Fever and South American Hemorrhagic Fever and contrary to Filoviruses these viruses do not cause endothelial cell damage, although little is known about how arenaviruses cause vascular permeability (1, 82, 90). Pro-inflammatory cytokines are elevated and there is a correlation between levels of TNFα and mortality (82, 90). A mouse model for arenaviruses has shown that arenavirus infection causes a loss of cellular function, but without causing damage to the cell or altering endothelial cell viability (82). Old World Arenaviruses bind the α-dystroglycan receptor (α-DG), a highly conserved and ubiquitously expressed cell surface receptor that binds ECM proteins. Studies have shown that arenaviruses downregulate the expression of a functional α-DG receptor resulting in a loss of communication between the cell and the ECM (90). New World arenaviruses recognize the Transferrin receptor 1 (TfR1) for cell entry, a receptor expressed on the cell surface of immune cells and vascular endothelial cells. Arenavirus binding to

either α-DG receptor or TfR1 may explain the pathogenesis observed in people infected with arenaviruses (90).

Flaviviruses:

Dengue virus causes increased vascular permeability without obvious damage to the endothelium (7). The mechanism behind dengue virus permeability changes is still not understood although increased patient cytokine responses are suggested to be the main cause (7, 82). Recent reports however, have also suggested a role for β_3 integrins and VEGFR2. β_3 integrins are required for Dengue virus infection in human endothelial cells and the severity of plasma leakage and viral load was inversely correlated with plasma soluble VEGFR2. Thus β_3 integrins and VEGFR2 may contribute to permeability during Dengue virus infection (7).

Viruses that use β3 integrins as cell entry receptor

Besides hantaviruses, several other viruses recognize $\alpha_v\beta_3$ integrins and use integrins for cell attachment and cell entry (102). In fact, $\alpha_v\beta_3$ integrins are among the most commonly used receptors by viral pathogens and their interaction with $\alpha_v\beta_3$ integrins can transmit cell signaling events that facilitate viral entry and infection (102).

Adenoviruses use the CAR (Coxsackie-adenovirus-receptor) receptor for cell attachment and αvβ3 integrins receptors for cell entry (22). However, in contrast to hantaviruses, adenoviruses bind integrins through penton base encoded RGD motifs and enter through classical receptor clustering and internalization paradigms (22,

102). Foot and Mouth Disease Virus (FMDV) (*Picornaviridae*) similarly contains an RGD motif on its capsid protein and uses $\alpha_v\beta_{6,}$ $\alpha_v\beta_{1,}$ $\alpha_v\beta_{3,}$ and $\alpha_v\beta_8$ integrin as cellular receptors (73, 102). FMDV usage of integrins does not seem to be associated with pathogenesis but is linked to tissue tropism (73).

Human cytomegalovirus (HCMV), a herpesvirus, also uses multiple receptors for viral entry (102, 123). HCMV reportedly binds to heparan sulfate, proteoglycans, β_1 integrins and $\alpha_v\beta_3$ integrins (102, 123). Binding to $\alpha_v\beta_3$ occurs through an RGD sequence in viral glycoproteins and initiates activation of cell signaling molecules such Src and Focal adhesion Kinase (FAK) which promote virus entry and infection (123). However, it is unclear whether $\alpha_v\beta_3$ integrin binding plays a role in herpes virus pathogenesis.

Section 2: Integrins

Integrins are heterodimeric transmembrane receptors consisting of non-covalently bound α and β subunits (46, 92). Nineteen α and eight β subunits have been characterized and at least 24 heterodimeric combinations have been identified. Integrins serve as anchoring molecules attaching the cell to the extracellular matrix and play a role in fundamental processes such as cell proliferation, cell differentiation, angiogenesis, immune cells regulation, platelet aggregration and cell migration (46, 92). There are only two integrins which contain the β_3 integrin subunit: $\alpha_{IIb}\beta_3$, which is the most abundantly expressed receptor on platelets (~80,000 copies /platelet) and $\alpha_v\beta_3$ which is mainly expressed on endothelial cells (92).

Integrin Bidirectional Signaling

Integrins connect the inside of the cells with the ECM and their ability for bi-directional signaling (outside-in and inside-out) is vital for normal cellular functions (46). Outside-in signaling events are changes in the ECM that require the cell to respond to their altered environment (46, 67). Integrins transmit signals for cell shape changes, integrin localization, intracellular pH changes, induction of protein phosphorylation and gene transcription (46). However inside-out signals are also directed by events within the cell that change the extracellular conformation of the integrin and alter ligand binding affinities, cellular adhesion, migration, growth and

differentiation (46, 67). As a result communication between the ECM and the cell is tightly controlled through structural rearrangements of cellular integrins (67).

Integrins exist in two conformations, an extended active integrin conformation and a bent inactive integrin conformer (Figure 2). Conformational states have primarily been studied using the crystal structures of αIIbβ3 and αvβ3 integrins (67, 105). The extended integrin conformation contains the ligand binding pocket at the apex of the integrin and is linked to integrin activation and high affinity ligand binding (46, 133). In contrast, in the bent conformation the ligand binding pocket is folded towards the cell membrane and the bent conformer is associated with a low ligand binding affinity (46, 133). The inactive integrin is bent at the "genu" of the integrin formed by the PSI domain, the hybrid domain and two of the EGF-like repeats (105, 133).

The PSI domain comprises the N-terminal 54 amino acids of the mature β_3 subunit (46, 129). PSI domains derive their names from the homology of plexins, semphorins and integrins (46) based on the relative position of 6-8 cysteines and a tryptophan residue (129). The β_3 integrin PSI domain has 7 cysteines which form 3 internal disulfide bonds (C5-C23, C16-C38, C26-C49), Cys13 forms a long disulfide bond with Cys435 (97). The PSI domain forms a double-stranded anti-parallel β sheet with two flanking short helices which are connected to the β sheet by disulfide bonds (97, 129). The W25 side chain forms a small hydrophobic core and Leu33 is located in the loop between two strands of the β sheet (129). Although the exact function of the PSI domain is unknown, it is believed that the PSI domain together with the

hybrid and two EGF-like repeats acts as a conformational switch that determines the movement of the head and leg domains of the integrin (97, 129).

The bent, inactive integrin conformation is the basal state of integrins expressed on cells (67, 133) with the ligand binding domain masked from the extracellular matrix. The PSI domain is at the apex of the bent integrin (5, 105, 133). Binding to the ECM (outside-in) or binding of cytoskeleton proteins to the integrin cytoplasmic domains (inside-out) results in a conformational change of the bent integrin into an extended conformation which binds ligands with high affinity (67) (Figure 2).

Integrins and Their Role in Vascular Permeability

Endothelial cells line the vasculature of every organ in the body and form a barrier between the vessel lumen and the surrounding tissue (128). The endothelium regulates blood flow, hemostasis, nutrient distribution, immune cell extravasation (14) inflammation, coagulation, wound healing and angiogenesis (42, 128). Angiogenesis involves the formation of new blood vessels and is mediated by endothelial cell specific growth factors like vascular endothelial cell growth factor (VEGF) (77, 118). VEGF has many effects on endothelial cells and plays a role as a unique growth factor which induces cell division in addition to its ability to dissociate endothelial cell contacts and permit endothelial cell migration required for vascular repair.

VEGF was originally identified as a vascular permeability factor which potently induced edema and was 50,000 times more effective than histamine in

directing fluid into tissues. VEGF binding to the VEGFR-2 receptor induces the internalization of VE-cadherin which is a unique endothelial cell adherence junction protein and forms the primary inter-endothelial cell fluid barrier. VEGF is released by platelets, immune cells and endothelial cells following vascular damage or changes in the ECM adherence (77). Endothelial cell migration is an essential step in angiogenesis and $\alpha_v\beta_3$ integrins serve a primary role in directing cell migration required for angiogenesis (77). Cell migration requires VEGF directed dissociation of adherence junctions which permits cell movement but also enhances capillary permeability. This is balanced by integrins which regulate VEGF permeabilizing responses by providing additional adherence functions and the direction of endothelial cell movement. VEGF and $\alpha_v\beta_3$ work in concert, in fact the ectodomains of VEGFR-2 and $\alpha_v\beta_3$ form an immunoprecipitable complex that coordinately regulates vascular permeability (9). The regulatory action of $\alpha_v\beta_3$ integrins and VEGFR-2 on angiogenesis and cell migration is also supported by studies of β_3 integrin deficient endothelial cells and mice (89). β_3 integrin knock-out mice are viable and their vasculature is indistinguishable from wild type mice. However, these mice present with reduced platelet function and microvascular hemorrhage suggesting that there are distinct differences in vascular permeability. Interestingly, β_3 integrin knock-out mice and endothelial cells in culture are hyper permeabilized by VEGF addition (89). These findings illustrate the intertwined role of $\alpha_v\beta_3$ integrins and VEGF in regulating capillary permeability and barrier functions (89, 99).

β_3 Integrins and Disease

Glanzmann Thrombasthenia (GT): Glanzmann's Thrombasthenia is a rare autosomal hereditary hemorrhagic disorder caused by the reduction or complete absence of platelet aggregation (91, 92). Patients with GT have prolonged bleeding times due to defective platelet function and adherence to the endothelium (92). GT stems from mutations in either α_{IIb} or β_3 subunits that result in either little or no expression of a functional $\alpha_{IIb}\beta_3$ integrin on platelets (16, 92). Mutations in the β_3 subunit lead to deficiencies in both $\alpha_{IIb}\beta_3$ and $\alpha_v\beta_3$ integrin and affect both platelet and endothelial cell functions. Interstingly, β_3 integrin knock-out mice serve as models of Glanzmann's Thrombastenia (16, 41, 91). Like GT patients, β_3 integrin knock-outs have classical symptoms of GT disease including prolonged bleeding times, impaired platelet aggregation, and microvascular hemorrhage (41, 91).

Fetomaternal Alloimmune Thrombocytopenia (FMAIT) and Post Transfusion Purpura (PTP)

β_3 integrins contain Human Platelet Antigens (HPA) which antigenically characterize platelet subtypes in human populations. Differences in HPA-1a and HPA-1b are derived by a single T-C nucleotide change which generates two β_3 integrin alleles and is specified by a single amino acid change within the β_3 integrin PSI domain. HPA-1a contains leucine at position 33, while residue 33 is a proline in HPA-1b individuals. The HPA-1b allele is present in 15-20% of the Caucasian population, ~ 8% of African populations and less than 1% of the Asian population (50). HPA-1a/b changes are antigenically important since they elicit immune

responses following transfusion, or direct maternal antibodies against fetal $\alpha_{IIb}\beta_3$ integrins with a different HPA-1 type. The incompatibility between mother and fetus can lead to severe fetal thrombocytopenia, fetal intracerebral hemorrhage and death in utero (49, 50, 117). Neonatal thrombocytopenia is seen in otherwise healthy newborns and occurs at a frequency of 0.9% in the general population. Within Caucasian populations, severe thrombocytopenia due to anti-HPA1 antibodies occurs in approximately 1 in 1000 pregnancies (50). Studies have shown that anti-HPA1a antibody binding to β_3 integrins leads to downstream signaling differences (49). Anti-HPA-1a antibodies inhibit fibrinogen binding by platelets thereby inhibiting aggregation of L33/L33 positive platelets and retarding or partially inhibiting the aggregation of L33/P33 platelets. In addition, anti-HPA1a antibodies reduce endothelial cell spreading and the negatively affected endothelial cell monolayer causes redistribution of junction proteins (49, 117).

Post-Transfusion Purpura or PTP is a rare but serious complication of blood transfusion and is caused by antibody responses to L33/P33 amino acid differences within the PSI domain of β_3 integrin (124). Patients homozygous for HPA-1b who receive blood from a homozygous HPA-1a donor form antibodies that destroy both donor and self platelets. The destruction of transfused and self platelets leads to severe thrombocytopenia approximately ten days after transfusion and last several weeks (124). Transfusion seems to trigger a recall response of HPA-1 antibodies in individuals who are already sensitized, e.g. women sensitized by pregnancy and men immunized through earlier transfusions (124). These findings demonstrate the

importance of β_3 integrins and PSI domain residues in thrombocytopenia and autoimmune responses.

Drug-Induced thrombocytopenia

ReoPro, Tirofiban, Eptofibatide and Quinine: ReoPro is a chimeric murine/human Fab fragment directed against β3 integrin. ReoPro binds to an epitope near to the β3 integrin ligand binding site and thus inhibits β3 integrin activation (10, 16). ReoPro was developed by Barry Coller at Stony Brook University and approved by the FDA in 1994 (16). Reopro prevents platelet-platelet adherence and ReoPro is given to patients following myocardial infarction or cardiovascular surgery to prevent coagulation that may occlude vessels. About 1% of patients receiving ReoPro for the first and 10 % of patients receiving ReoPro for the second time will develop acute and severe thrombocytopenia 5 - 8 hours after administration of the drug (6, 10). In both cases thrombocytopenia is believed to be caused by antibodies that recognize either murine sequences incorporated into ReoPro or conformational changes caused by binding of Reopro to the β_3 integrin on platelets (10) (6).

Tirofiban and Eptofibatide are two ligand mimetic drugs for $\alpha_{IIb}\beta_3$ integrin. They occupy the RGD recognition site of $\alpha_{IIb}\beta_3$ integrin thereby preventing fibrinogen binding to $\alpha_{IIb}\beta_3$ integrin (6). As with ReoPro, a subset of patients will develop severe thrombocytopenia after administration of the ligand-mimetic drugs and studies indicate that thrombocytopenia is caused by antibodies that recognize the ligand-mimetic occupied $\alpha_{IIb}\beta_3$ (6). The epitopes for antibody recognition in drug dependent thrombocytopenia are not known except in the case of quinine induced

thrombocytopenia (83). Quinine is a small molecule with anti-inflammatory and fever reducing properties and used to be the antimalarial drug of choice. A subset of people taking quinine develops quinine induced thrombocytopenia and studies have shown that quinine dependent antibodies bind to residues 50-66 of the β_3 integrin subunit. This region overlaps the hybrid and PSI domains of β_3 integrin and disulfide bonds required to stabilize the target epitope (83).

Heparin: Heparin-induced thrombocytopenia and thrombosis (HITT) is caused by the formation of antibodies against Heparin-Platelet Factor 4 complex. Heparin-PF4 complexes form on slightly activated platelets followed by binding of IgG which binds to heparin-PF4 complex on the platelets through the Fab region. Subsequently, the Fc region of the IgG binds to the Fcgamma Receptor II (FcγRII) in an autocrine and paracrine manner and strongly activates platelets. As a result, more PF4 is released from the activated platelets and available for heparin binding (10, 37). Platelet activation results in the formation of platelet microparticles and blood clots which leads to a decrease in platelet count (10). Aggregation of platelets is dependent on $\alpha_{IIb}\beta_3$ integrin and studies have shown that HIT positive individuals, who are also HPA-1b positive, have an associated increased risk of thrombosis (37).

Diseases such GT, FMAIT, PTP and drug-induced thrombocytopenia demonstrate that β_3 integrin dysfunction is caused by mutations or antibodies targeting the β3 integrin and have prominent effects on platelet and endothelial cell functions. Interestingly, individuals infected with hantaviruses develop similar symptoms to patients suffering from GT, FMAIT, PTP and drug-induced

thrombocytopenia. Hantaviruses keep $\alpha_v\beta_3$ integrins in a bent inactive state by binding to the β_3 PSI domain. This is the same domain which defines the HPA-1 polymorphism and determines FMAIT and PTP immune responses (86). Hantaviruses block β_3 integrin directed cell migration and like β_3 integrin knockouts, also direct the hyperpermeability of endothelial cells in response the VEGF (27, 28). Therefore, hantavirus interactions with β_3 integrins mirror the effects of β_3 integrin dysfunction and provide a compelling rationale for hantavirus-β_3 integrin interactions to contribute to vascular permeability and HPS and HFRS pathogenesis.

Chapter 2:

Experimental Procedures

Cells and Virus

Vero E6 cells (African Green Monkey Kidney Epithelial Cells) (ATCC CRL 1586) and CHO (Chinses Hamster Ovarian Cells) cells were grown in Dulbecco's Modified Eagle Medium (DMEM) containing 10% fetal calf serum (FCS, 56^0C inactivated), penicillin (100 mg/ml), streptomycin sulfate (100 mg/ml), and amphoterecin B (5 mg/ml) (GIBCO). BHK 21 (Baby Hamster Kidney) cells (ATCC CCL-10) were grown in Glasgow Minimum Essential Medium (GMEM) supplemented with Tryptose Phosphate Broth solution (Sigma) and with 100 mM nonessential amino acids (GIBCO). Andes virus (CH1-7913) (23) was kindly provided by Dr. B. Hjelle (Department of Pathology, School of Medicine, University of New Mexico, Albuquerque). HUVECs (Human Umbilical Vein Endothelial Cells) (Clonetics) were grown in endothelial cell basal medium-2 (EBM-2) supplemented with human recombinant epidermal growth factor (10 ng/ml), hydrocortisone (1 μg/ml) gentamicin (50 μg/ml) amphotericin B (50 μg/ml) (GIBCO), 0.1% endothelial growth factor and 2% FCS (Clonetics). ANDV and NY-1V were cultivated in a biosafety level 3 facility (BSL3) as previously described (27). Briefly, viruses were adsorbed onto Vero E6 or BHK-21 cells monolayers for 1 hour at a multiplicity of infection (MOI) of 0.5, washed, and grown in maintenance medium DMEM or GMEM with 2% FCS.

Bacterial strains

The following bacterial strains were used:

XL1Blue: recA1 endoA1 gyrA96 thi-1 hsd R17 supE44relA1 lac[F' proAB laqIPZΔM15Tn10 (Tet^R)] (Stratagene).

BL21(DE3): F-ompT $hsdS_B(r_B\text{-}m_B\text{-})$ gal dcm (DE3) (Novagen).

Antibodies

Anti Polyclonal rabbit sera to α_1 (Ab 1934), α_2 (Ab 1930), β_3 (Ab 1932), $\alpha_5\beta_1$ (Ab 1950), and blocking monoclonal antibodies to β_2 (MAb 1962) and to $\alpha_v\beta_3$ (MAb1976) were from Chemicon International Inc. Goat anti-rabbit horseradish peroxidase conjugate and fluorescein labeled Goat anti-mouse IgG(H+L) were from Kirkegaard and Perry Laboratories, Inc. The generation of rabbit antisera to the hantavirus nucleocapsid protein was previously described (27). Briefly, anti-N-protein specific polyclonal rabbit serum made to recombinant N-protein from NY-1V expressed in Escherichia coli (29). N-protein-specific sera cross-reacts with N-protein from all tested hantaviruses (29). Antibodies to synthetic peptides of human β3 integrin were generated by immunizing chickens three times with a peptide containing β_3 integrin residues 17-48 conjugated to KLH (Invitrogen). Purification of immune and control yolks were performed with Eggcellent TH Chicken IgY purification kit (Pierce) according the manufacturer's instructions. Non-immune rabbit sera and yolks were used as negative controls.

Polymerase Chain Reactions (PCR)

PCR reactions were performed in an Eppendorf Personal Mastercycler. Each reaction consisted of 1X buffer (50 mM Tris-HCl, pH 9.0 and 20 mM $(NH_4)_2SO_4$, 2.5 mM $MgCl_2$, 0.2 mM dNTPs (USB), 1 U *Tfl* polymerase (Epicenter) forward and reverse primers (100 ng each primer) and 10-100 ng template. Annealing temperatures used varied from 50-60°C depending on template DNA and oligo. A generic cycle used for amplying PCR products is as following: denaturation at 95°C for 30 seconds, annealing for 30 seconds and elongation at 72°C for 1min/kb of PCR product.

RNA/cDNA

Total RNA was extracted from Syrian hamster cell line BHK-21 and Syrian hamster liver tissue (RNAeasy, Qiagen). Tissue was lysed with 0.5 ml of a guanidine based lysis buffer (buffer RTL + β-mercaptoethanol). Lysates were purified according to manufacturer's instructions. Briefly, one volume of 70% ethanol was added to the lysate and the lysate was passed through an RNAeasy column. The column was washed with 2 volumes of RPE buffer and RNA was eluted in RNAse-free water. 1 μg of RNA was used to prepare template cDNA (Roche) with primers based on conserved sequences within human, murine, rat and rabbit β3 integrin integrins (GenBank accession nos. NM_00012, NM_016780, NM_153720 and NM_001082066 resp.):

antisense primers 5'ATCACAKACTGTAGCCTGCATGATGGC 3', ending at 777 and 5'AGCACRTGTTTGTAGCCAAACATGGG 3', ending at bp 659, R= A or G, K= T or G (cycle 25°C 10 min, 42°C 60 min, 95°C 5 min). The obtained fragments were subjected to a nested PCR using forward primer:

5' CTGGCGCTGGGGGCGCTGGCGGGCGT 3' starting at bp 43 and the reverse primer : 5' TCCACRAAKGCCCCRAAGCCAATCCG 3' ending at bp 551 (cycle 95°C 1 min., 60°C 1 min., 72°C 30 sec.). The obtained DNA fragment was ligated into pCRIITOPO (Invitrogen), transformed into XL1Blue and sequenced. The region corresponding to the N-terminal 53 residues of human β3 integrin was subcloned into pET6His vector, transformed into BL21(DE3) cells and subsequently expressed.

Restriction digestions

Digests were performed in 50 μl reactions at 1X concentrations of provided buffers. Enzymes were purchased from New England Biolabs (NEB) or Invitrogen and buffers were used according to manufacturer's suggestions. For screening reactions, 1-2 U of enzyme was used per reaction and digested for 1 hour at 37°C. For cloning, 2 μg of DNA was digested with 10 U of restriction enzyme for 1 hour at 37°C.

Gel purification

Digested PCR products and vectors were run on a 1% agarose gels containing ethidum bromide (Ultrapure Agarose, Invitrogen) in TAE buffer (40mM Tris acetate and 10mM EDTA, pH8.0) at 100 V. After sufficient separation, bands were excised and placed in an Eppendorf. DNA was purified using the Qiagen Gel Extration Kit according to manufacturer's instructions. Gel slices were dissolved in QB buffer and melted at 50°C for 10 minutes. The mixture was added onto a column and centrifuged for 1 min at >10,000 rpm. Columns were washed with ethanol buffer and eluted with Tris buffer (pH 8.0) or water.

DNA ligation

For each ligation, a 20 µl reaction was set up containing the following: insert DNA, vector DNA, T4 DNA ligase buffer (1X buffer: 50mM Tris-HCl (pH 7.6), 10mM Mg Cl_2, 1 mM DTT, 1 mM ATP, 0.5% polyethylene glycol 8000) and T4 DNA ligase (1U). The reaction was mixed and allowed to incubate overnight at 16°C.

Site-directed mutagenesis

Stratagene's QuikChange Site-Directed Mutagenesis kit was used for β_3 integrin mutation reactions according to manufacturer's protocols. Reactions contained 5 µl of 10X Reaction buffer (1X reaction: 10 mM KCl, 10 mM (NH4)SO4, 20 mM Tris-HCl (pH8.8), 2 mM MgSO4, 0.1% Triton-X-100, 0.1 mg/ml BSA, 50 ng

DNA, 125 ng forward primer and reverse primers, 1 µl *Pfu Turbo* polymerase (elongation rate ~1 kb per minute). Amplifications took place under following conditions: 95°C (30 seconds), 1 cycle; 95°C (30 seconds); 55°C (1 min), 68°C (1-3 min), 16 cycles; 4°C, hold.

After the cycle was completed, 1 µl *DpnI* was added to each reaction and incubated at 37°C for 1 hour to digest template plasmid. 1 ml of each reaction was transformed into chemically competent XL1 Blue cells by incubation on ice (30 min) and heat shocked at 42°C for 45 Sec. Transformed cells were incubated in 500 µl LB for one hour at 37°C and spread on LB plates containing antibiotics.

Preparation of competent cells

XL1 blue and BL21(DE3) competent cells were transformed by electroporation and prepared as follows. Cells were grown overnight and diluted 1:50 in 1000 ml of fresh Luria broth (LB; 1% NaCl-1% tryptone-0.5% yeast extract, pH 7.0) and grown at 37°C to an A_{600nm} of 0.6. Cells were pelleted in a Sorvall Superspeed centrifuge at 5000 rpm for 5 min and pellets were washed with ice-cold sterile water. Washes and spins were repeated four times. After a final wash, cells were washed once in 10% ice-cold glycerol, pelleted for 15 min at 3500 rpm and resuspended in 1 ml of 10% glycerol. Cells were aliquoted in 50 µl per 1.5 ml tube, and flash-frozen in a dry ice/ethanol bath. Cells were stored at -80°C until use.

Bacterial Transformation

For transformation, frozen XL1 blue or BL21 (DE3) competent cells were thawed on ice, 1-2 µl (~0.1-10 ng) DNA was added, and cells were transferred to a pre-chilled 0.1 ml cuvette (Invitrogen). Cells were electroporated using a Bio-Rad gene pulsar (200 ohms, 25 µF, 1.25 kV). Six hundred µl of pre-warmed (37°C) LB was immediately added to cells, which were incubated for recovery at 37°C for 1 hour with shaking. To obtain bacterial colonies containing the plasmid of interest, transformed cells were plated on LB agar plates with the appropriate antibiotic(s), and incubated at 37°C overnight.

Preparation of Plasmid DNA

Alkaline Lysis Mini-prep*:*

A 3 ml LB culture was grown overnight at 37°C with shaking. Cells were pelleted at >12,000 rpm for 2 min and resuspended in 100 µl Solution I (50 mM glucose, 25 mM Tris pH 8.0, 10 mM EDTA, + RNase A). Cells were lysed in 200 µl Solution II (200 mM NaOH, 1% SDS) at room temperature for 1 min and subsequently neutralized with 150 µl Solution III (3 M potassium, 5 M acetate) to precipitate protein and genomic DNA. The prep was centrifuged at >12,000 rpm for 10 min at room temperature. The cleared lysate was moved to a clean tube and the pellet discarded. The mixture was phenol/chloroform extracted once: an equal volume of cold phenol/chloroform was added to the supernatant and vortexed for one minute.

The mixture was centrifuged at >12,000 rpm to separate phases and the upper aqueous layer was removed to a clean tube for ethanol precipitation: 1/10 volume of 3M sodium acetate pH 5.2 and 2.5 volumes of ethanol and were added the aqueous layer. The sample was vortexed and stored at -80°C for 10 minutes to allow DNA to precipitate. DNA was pelleted at 14,000 rpm for 10 minutes and the resulting supernatant was discarded. The pellet was washed with 70% cold ethanol and resuspended in 50 µl 10 mM Tris-HCL pH 8.0 or distilled water and 1 µl of RNase A (10 mg/ml) was added.

Cesium Chloride Maxi Prep:

A 500 ml LB culture was grown overnight at 37°C with shaking. Cells were pelleted at 5000 X g for 5 min and resuspended in 6.5 ml of Solution I (50 mM Glucose, 25 mM Tris-HCl pH 8, 10 mM EDTA). The cells were lysed with 13.5 ml of Solution II (0.2 M NaOH, 1% SDS) for 5 minutes on ice. The lysate was neutralized with 10 ml of Solution III (3 M Potassium Chloride, 5 M Acetate) for 5 minutes on ice and spun at 3500 rpm in a tabletop centrifuge for 30 min at 4°C. 20 ml of isopropanol was added to the supernatant and incubated at room temperature for 30 minutes. DNA was pelleted at 3500 rpm for 30 minutes in a tabletop centrifuge. The pellet was washed in 3 ml of 70% ethanol, dried and resuspended in 4 ml of TE pH 8.0. Exactly 4.4 g of CsCl and 10 µl of ethidium bromide (10mg/ml) was added and the mixture was sealed in a polyallomer Quik-Seal tube (13 x 51 mm) (Beckman). The sample was spun in a vTi65 rotor at 50,000 rpm, 18 hours in a Beckman LS-70

ultracentrifuge. Plasmid DNA bands were harvested by side puncture using a 20G needle. DNA was extracted with butanol saturated water (5 x 3 ml) to remove ethidium bromide. The sample was dialyzed overnight in TE using 14 kDa MWCO dialysis tubing to remove the CsCl. DNA was recovered by ethanol precipitation.

Plasmids

cDNA coding regions for human β_3 and α_v, murine β_3 and bovine β_3 integrin subunits were previously cloned in pcDNA3.1(-)/ZEO. Bovine β_3 P33L and human β_3 L33P mutants were generated by oligonucleotide-directed mutagenesis as described above (Stratagene) and sequenced. Clones containing residues 1-53 of human β_3, bovine β_3, bovine β_3 P33L and murine β_3 were subcloned from full length human, bovine and murine β_3 plasmids into pET6His at the BamH1/EcoRI site as previously described (86).

Mammalian cell transfection

Lipofectamine 2000: Transfections were performed on monolayers of CHO cells (~75-95% confluent) in 6-well plates (Corning, Inc) using Lipofectamine 2000 (Invitrogen) according to manufactures instructions. Briefly, cells grown in one well of a 6-well plate were transfected using a 3:1 ratio (v/w) Lipofectamine 2000 to plasmid DNA (0.5 μg each) per well for 16 hours. Monolayers were washed with 1X PBS, and grown in complete DMEM (10% FCS, penicillin and streptomycin) for 48 hours prior to analysis.

Flow cytometry

CHO cells were transfected (Lipofectamine 2000, Invitrogen) as recommended with equal amounts of human α_v and either human β_3 or bovine β_3 expression plasmids (pcDNA3.1). Two days post transfection, transfected CHO cells were washed with ice-cold PBS and cells were dissociated with enzyme-free PBS based cell dissociation buffer (Invitrogen). Cells were resuspended in 100 µl of PBS 2% FCS and incubated with anti-$\alpha_v\beta_3$ (mAb 1976) (2 µg per 1 x 10^6 cells) for 30 minutes at 4°C. Cells were pelleted (1000 rpm for 2 minutes), washed twice with ice cold PBS and incubated with anti-mouse FITC for 30 minutes at 4°C. Cells were repelleted, washed twice with ice cold PBS 2% FCS, resuspended in 500 µl PBS and subjected to flow cytometry (FACSCalibur cell sorter, BD Biosciences). The geometric mean titer of β_3 integrin fluorescence on CHO cells was used as measure of integrin expression levels and only cells expressing comparable levels of human or bovine β_3 integrins were used in ANDV infection experiments.

Protein expression and purification

Isopropyl-β-D-thiogalactopyranoside (IPTG) induction (1 mM for 3 hours) of pET6His plasmid in BL21(DE3) cells was used to express β_3 polypeptides containing residues 1-53 and performed at 30°C as previously described (86). Briefly, 50 ml bacterial pellets were resuspended in 0.1 M NaH_2PO_4/10 mM Tris-HCl/ 1 M urea, sonicated, and purified on Ni^{2+}-NTA resin (Qiagen). Proteins were eluted with 50

mM EDTA, dialyzed overnight in PBS (3.5-kDa cutoff), and protein concentrations were quantitated by bicinchoninic acid (BCA) assay (Pierce).

Immunoprecipitation Assays

CHO cells were transfected with plasmids expressing Human αv and either human β_3, human β_3 L33P, bovine β_3 or bovine β_3 P33L. Two days post-transfection, cells were washed with 1X PBS and lysed in RIPA lysis buffer (1% NP40, 0.5% Sodium deoxycholate, 0.1% SDS, leupeptin; 10 μg/ml, aprotinin ;10 μg/ml, pepstatin A; 1 μg/ml). Lysates were clarified by centrifugation and $\alpha_v\beta_3$ integrins proteins were immunoprecipitated with anti-$\alpha_v\beta_3$ MAb (LM609), and protein A/G-plus agarose beads. Beads were washed 5 times with RIPA lysis buffer and resuspended in non-reduced SDS sample buffer. Precipitated proteins were analyzed by Western blot as indicated.

Western Blotting

Purified β_3 polypeptides or immunoprecipated β_3 proteins were separated by 15% or 7% SDS-PAGE respectively. Proteins were transferred in a cold Tris-Glycine transfer buffer (30 % methanol) to nitrocellulose using a Novex Xcell electroblotter for 1 hour at 100V and blocked with 2% BSA. Full length β_3 proteins were detected using rabbit anti-β_3 antibody (MAb1932, Chemicon) (1:2,000) or chicken antibodies made to a purified human β_3 polypeptide containing residues 17-48. Blots were

washed 3 times with 1X Tris-buffered saline (TBS-T; 50 mM Tris, 150 mM NaCl, pH 7.4, 0.4% Tween 20) and incubated with anti-rabbit (1:5000) (Amersham) or anti-chicken (1:2000) (Kirkegaard) HRP-conjugated antibody. Western Blots were developed by fluorography in the presence of ECL reagent (Amersham).

Silver Staining

Silver staining reagents were purchased from Biorad and the staining was performed according to the manufacturer's protocol. Briefly, the gel was methanol fixed in Fixation Solution I (40% methanol, 10% acetic acid) for 30 minutes followed by two 5 minutes washes of Fixation Solution II (10% ethanol, 5% acetic acid). Proteins were oxidized for 5 minutes using a 1X Oxidizing Solution. Washed 5-8X with distillled water and then incubated with 1X Silver Solution for 20 minutes. Two 30 second incubations with Developing Solution were used to develop bands. The reaction was terminated with Stop Solution (5% acetic acid).

Ligand and Antibody Pretreatment of Cells

HUVECs, VeroE6 cells and BHK-21 cells were pretreated with antibodies (0.1 µg/ml-1 µg/ml) or potentially competitive ligands (5 µg/ml - 20 µg/ml) for 1 hour at 4°C. Antibodies and ligands were pre-adsorbed to cells in 50 µl of DMEM with 2% FCS in duplicate wells of a 96-well plate on ice. Sera or ligands were removed and cells were washed with PBS. Approximately 1000 focus forming units of hantavirus were adsorbed to monolayers for 1 hour at 37° C. Unbound virus was removed,

monolayers were washed three times with PBS and infected monolayers were incubated 24 hours prior to methanol fixation (100% methanol, 30 minutes at -20° C).

Polypeptide Inhibition of Hantavirus Infection

Increasing amounts (5 μg/ml - 20 μg/ml) of human (Hu), murine (Mu), bovine (Bo), P33L bovine mutant (Bo P33L) or Syrian hamster (Syr. Ham.) β_3 polypeptides (residues 1-53) were incubated with approximately 1000 FFUs of ANDV or NY-1V (2 hours at 4°C). Subsequently virus was adsorbed to VeroE6 cells or BHK-21 cells in duplicate wells (96 well plate, 100 μl per well) for 1 hour at 37°C. Monolayers were washed with PBS and cells were grown in complete media for 24 hours prior to methanol fixation. Nucleocapsid protein present in infected cells was detected by immunoperoxidase staining using anti-nucleocapsid antibody and the number of N-protein containing cells was quantitated as previously described.

Cloning and Sequencing of Syrian Hamster β_3 Integrin Subunit

Total RNA was extracted from Syrian hamster cell line BHK-21 and Syrian hamster liver tissue (RNAeasy, Qiagen). RNA was reversed transcribed into cDNA (Transcriptor First Strand cDNA Synthesis, Roche) (25°C 10 min, 42°C 60 min, 95°C 5 min) using primers containing consensus β_3 integrin subunit sequences derived from human, murine, rat and rabbit β_3 integrins: antisense primers 5'ATCACAKACTGTAGCCTGCATGATGGC 3', ending at bp 777 of human β_3

integrin sequence and 5'AGCACRTGTTTGTAGCCAAACATGGG 3', ending at bp 659 of the human β_3 integrin sequence, R= A or G, K= T or G. cDNA was subjected to nested PCR using a forward primer 5' CTGGCGCTGGGGGCGCTGGCGGGCGT 3' starting at bp 43 of the human β_3 integrin sequence and the reverse primer 5' TCCACRAAKGCCCCRAAGCCAATCCG 3' starting at bp 526 of the human β_3 integrin sequence (cycle 95°C 1 min., 60°C 1 min., 72°C 30 sec.). Amplified cDNA fragments were ligated into pCRII-TOPO (Invitrogen), transformed into XL1Blue cells and sequenced. The region corresponding to the N-terminal 53 residues of human β_3 integrin was subcloned into pET6His vector at the BamHI/EcoRI site, transformed into BL21(DE3) cells and subsequently expressed as described above.

CHO cells transfection and infection

CHO cells were transfected (Lipofectamine 2000, Invitrogen) as recommended with equal amounts of human α_v and either human β_3 or bovine β_3 expression plasmids. Two days post transfection, $\alpha_v\beta_3$ integrin expression was detected by flow cytometry as described above. Transfected and mock transfected CHO cells were infected with ANDV 48 hours post transfection as described above. Cells were methanol fixed after 24 hours, immunoperoxidase stained for hantavirus nucleocapsid protein, and the number of infected cells was quantitated by microscopy as previously described (86).

Quantitation of Hantavirus-infected cells

Methods for immunoperoxidase staining of hantavirus antigens in infected cells were previously described (29). Cell monolayers were fixed in 100% methanol for 20 min at -20^{0}C and incubated with polyclonal rabbit anti-nucleocapsid serum (1/2000) for 1 h at 37^{0}C. Monolayers were washed four times with PBS and incubated with 1/2000 dilution of goat anti-rabbit horseradish peroxidase conjugate (Kirkegaard & Perry Laboratories). Monolayers were then washed four times with PBS and stained with 3-amino-9-ethylcarbazole (0.026%) in 0.1 M sodium acetate (pH 5.2)-0.03% H_20_2 for 5 to 30 min**.** Reactions were stopped by washing with distilled water, and immunoperoxidase-stained infected cells were quantitated and compared to that of mock infected or untreated infected cell controls.

Chapter 3:

Results

ANDV infection of Syrian hamsters is the only model of hantavirus disease which mimics human HPS disease. However, infections of Syrian hamsters by other pathogenic hantaviruses have failed to cause disease. These findings and the ability of ANDV to spread from person to person suggest that ANDV has unique attributes that permit its spread and pathogenesis. Although all pathogenic hantaviruses studied thus far use human β_3 integrins, the use of β_3 integrins by ANDV has not yet been investigated and it is unclear whether β_3 integrins in Syrian hamsters confer susceptibility to any hantaviruses.

Replication of ANDV and NY-1V in BHK-21 Cells and VeroE6 Cells

Baby Hamster Kidney 21 cells (BHK-21 cells) are derived from Syrian hamsters and initially we determined whether ANDV enters BHK-21 cells similar to VeroE6 cells. Figure 3 indicates that the addition of identical amounts of ANDV to VeroE6 and BHK-21 cells resulted in the infection of both cell types although the number of infected VeroE6 cells was approximately 2-fold higher than BHK-21. In contrast, infection of BHK-21 cells by NY-1V was reduced by >3 logs compared to the infection of VeroE6 cells (Figure 3). This result suggests that there is a fundamental difference in ANDV and NY-1V infection of BHK-21 cells. This difference could occur through a number of mechanisms including receptor entry or post-entry events that permit successful ANDV infection

Inhibition of ANDV Infection with Vitronectin and Antibodies

Syrian hamsters infected with ANDV develop a lethal disease with onset, symptoms and respiratory distress similar to that of HPS patients. To date all pathogenic hantaviruses have been demonstrated to use β_3 integrins for cellular entry and pathogenic hantaviruses inhibit β_3 functions days after infection. However, ANDV interactions with human or Syrian hamster β_3 integrins have not been defined, and the role of β_3 integrins in regulating endothelial barrier functions provides a rationale for β_3 integrin contribution to viral pathogenesis.

Here we investigated whether ANDV interacts with human or Syrian hamster β_3 integrins and defined residues required for ANDV infection. Initially, we determined whether pretreating VeroE6 cells or Syrian hamster BHK-21 cells with specific ligands or antibodies to $\alpha_v\beta_3$ integrins inhibited ANDV infection. Pretreating cells with increasing amounts of collagen, chondroitin sulfate, laminin or fibronectin had no effect on ANDV infection. In contrast, pretreating VeroE6 cells (Figure 4A) and BHK-21 cells (Figure 4B) with vitronectin, a high affinity $\alpha_v\beta_3$ ligand, inhibited ANDV infection by 80% and 70% respectively. Unfortunately, antibodies that recognize Syrian hamster β_3 integrins are not available and antibodies to human β_3 integrins do not recognize Syrian hamster β_3 integrins (Figure 5). This permitted us to investigate only the ability of antibodies to human β_3 integrins to inhibit ANDV infection in HUVECs (Figure 6A) and VeroE6 cells (Figure 6B). Pretreating cells with antibodies to human β_3 or $\alpha_v\beta_3$ dose-dependently inhibits ANDV infection of HUVECs and VeroE6 cells (85% and 70%, respectively; Figures 6A and 6B).

Antibodies to the α_v integrin subunit also reduced ANDV infection of HUVECs and VeroE6 cells (40-60 %) while antibodies to α_1, α_2, β_2 and β_5 had no inhibitory effect on ANDV infection. These results indicate that ligands or antibodies specific to $\alpha_v\beta_3$ integrins block ANDV entry into human, simian and Syrian hamster cells.

Inhibition of ANDV with human PSI domain

NY-1V binding to β_3 integrins was previously shown to be RGD independent and mediated by the N-terminal PSI domain present on human, but not murine β_3 integrin subunits (29, 86) In order to determine if ANDV interacts with human β_3 integrin PSI domains, we determined whether expressed β_3 integrin PSI domain (residues 1-53) inhibited ANDV infectivity. Pretreating ANDV with increasing amounts of the expressed human β_3 PSI domain reduced ANDV infection of HUVECs by 75% (Figure 6A) and ANDV infection of BHK-21 cells by 85% (Figure 7B). In contrast, the murine β_3 integrin PSI domain had no apparent effect on ANDV infection of either cell type.

Minimal Domain Required for Hantavirus Recognition

The expressed polypeptide containing residues 1-53 comprises the N-terminal PSI domain of β_3 integrins and inhibits pathogenic hantavirus infection (86). Within the 1-53 N-terminal β_3 integrin there are 7 cysteine residues which form 3 internal disulfide bonds in β_3 integrins expressed on the surface of cells (5-23, 16-38 and 26-

49) (Figure 8). In order to determine the minimal domain required to inhibit ANDV infection, we synthesized small peptides between cysteine residues present in the human N-terminal β_3 integrin 1-53 domain. A peptide containing β_3 residues 13-49 has 6 cysteine residues but Cys13 forms a long range disulfide bond with Cys435. Only 2 paired cysteine residues, 16-38 and 26-49, remain in the β_3 integrin PSI domain containing residues 13-49. Peptide 17-48, contains 3 cysteines but no native disulfide bonding cysteine pairs and includes domains that differ between human and murine β3 (Figure 8).

In Figure 9, increasing amounts (5 μg–20 μg) of human β_3 polypeptides 13-49 or 17-48 were incubated with ANDV, NY -1V, HTNV or PHV prior to adsorption onto VeroE6 cell monolayers. Twenty four hours post-infection the number of infected cells was quantitated by immunostaining for the viral N-protein (Figure 9). Murine β_3 homologues were used as negative controls for the human β_3 peptide inhibition assay. Results show that human, but not murine, β_3 peptides containing residues 13-49 (Figure 9A) or 17-48 (Figure 9B) dose-dependently inhibited pathogenic hantavirus infection of VeroE6 cells whereas PHV infection is not inhibited by either peptide. These results suggest that shorter peptides within the β_3 integrin 1-53 PSI domain are functional in blocking pathogenic infection of cells. Additionally these studies are consistent with studies of bacterially expressed PSI domains in suggesting that peptide inhibition does not require native disulfide bonds within the β_3 integrin PSI domain.

Antibodies to PSI domain Inhibit Pathogenic Hantavirus Infection

Thus far, there are no antibodies that specifically target the β_3 integrin N-terminus which is the hantavirus interacting domain. However our results show that the human β_3 integrin 17-48 peptide inhibits pathogenic hantavirus infection of VeroE6 cells. As a result, we used the human β3 17-48 peptide to generate polyclonal antibodies to the PSI domain using a commercial antibody service (Biosynthesis). Purified antibodies made to 17-48 recognized the human β3 17-48 polypeptide as well as expressed human β_3 1-53, human β3 1-136 and full length β_3 as shown in Figure 10. Subsequently we used the anti-17-48 peptide sera in antibody inhibition assays to determine whether it inhibited infection by NY-1V, HTNV, PHV or ANDV (Figure 11 and 12). VeroE6 cells or HUVECs (figure 12B) were pretreated with increasing concentrations (0.01 μg, 0.1μg, 1μg) of the anti-17-48 antibodies and subsequently infected with NY-1V, HTNV, PHV and ANDV. Antibodies to $\alpha_v\beta_3$ and preimmune rabbit sera were used as positive and negative controls respectively. After 24 hours, infected cells were quantitated by immunostaining for the viral N-protein. Pretreating VeroE6 cells (Figure 11 and 12) and HUVECs (Figure 12B) with antibodies against the human β_3 integrin PSI domain resulted in a 70% to 90% decrease in pathogenic hantavirus infection compared to control antibodies. PHV was not inhibited by antibodies against human β_3 integrin PSI domain. However, as previously shown, PHV infection was blocked by antibodies against $\alpha_5\beta_1$ integrins. Figure 13 shows that antibodies against human β_3 integrin PSI domain recognizes

human, murine and bovine β_3 integrin PSI domain but not Syrian hamster β_3 integrin PSI domain. Therefore we could not analyze antibody inhibition of ANDV infection of BHK-21 cells.

Syrian hamster β_3 Integrin Sequence

Six independent clones of the Syrian hamster β_3 integrin PSI domain obtained from BHK-21 cells were sequenced. All clones were identical except for one clone which had an aspartic acid residue (D39) at position 39 while 5 others had an asparagine residues at this position (N39). In order to confirm this, we also extracted Syrian hamster β_3 integrin from Syrian hamster liver tissue and found that all 7 clones had an asparagine at position 39. Therefore, we concluded that the wild type Syrian hamster β_3 integrin PSI domain contains an asparagine at position 39. The mutant D39 clone of Syrian hamster β_3 (1-53) was used for comparative analysis in further experiments. Figure 14 compares the Syrian hamster β_3 integrin coding sequences with human, murine and bovine β_3 PSI domains. The Syrian hamster β_3 integrin PSI domain differs from human sequences by 8 residues. In contrast, murine and bovine PSI domains, which do not confer hantavirus infectivity, differ by 9 and 4 residues, respectively, from human PSI domains, while murine sequences differ by 5 residues from the Syrian hamster PSI domain (positions 30, 32, 42, 43, 50).

Inhibition of ANDV infection by the Syrian hamster PSI domain

Since ANDV infected BHK-21 cells efficiently, we evaluated whether the expressed Syrian hamster β_3 integrin PSI domain was capable of inhibiting ANDV infection. Figure 15 indicates that pretreating ANDV with the Syrian hamster β_3 integrin PSI domain (1-53) reduced ANDV infection of BHK-21 cells by 80%, similar to the human β_3 integrin PSI domain (1-53). In contrast, the murine β_3 PSI domain had no effect on ANDV infection of BHK-21 cells at any concentration. This indicates that both the Syrian hamster and human β_3 integrin PSI domains interact with ANDV and further suggest that ANDV infection of BHK-21 cells is β_3 dependent.

Since it was previously demonstrated that the presence of an N or D residue at position 39 of β_3 determined NY-1V interaction with β_3 (86), we determined whether mutating residue 39 of the Syrian hamster β_3 PSI domain from N to D altered the ability of the PSI domain to inhibit infectivity. However, Figure 15 indicates that there was no difference in PSI domain inhibition of ANDV between the N39 wt or the D39 mutant. This suggested a fundamental difference in the interaction of β_3 with ANDV and NY-1V at the level of PSI domain residues. In order to determine if the WT Syrian hamster β_3 or the N39D mutant Syrian hamster β_3 inhibited NY-1V infectivity we comparatively evaluated the ability of the NY-1V and ANDV to infect HUVECS in the presence or absence of β_3 PSI domains. Figure 16 demonstrates that both human and Syrian hamster β_3 PSI domains inhibited ANDV infection of human endothelial cells irrespective of the N39D mutation. In contrast, the Syrian hamster

WT β_3 PSI domain had no effect on NY-1V infection of endothelial cells while the Syrian hamster N39D mutant blocked NY-1V infectivity similar to the human β_3 PSI domain. This supports previous findings on the specificity of NY-1V interactions with β_3 (86) and indicates that ANDV interactions with β_3 integrins require discrete PSI domain residues from that of NY-1V.

Residue Differences Between β_3 Integrins of Different Species

Specific PSI domain inhibition of ANDV infection further suggests that PSI domain sequences determine ANDV attachment and infectivity. We previously determined that substituting residues 1-43 of murine β_3 with human β_3 sequences conferred hantavirus infection (86). Results described above show that peptides containing residues 17-48 of human β_3 integrin inhibit ANDV infection of VeroE6 and BHK-21 cells. When these findings are considered, only 2 residues in the murine β_3 (T30, S32) and 1 in the bovine β_3 (P33) are completely discrete from human or Syrian hamster PSI domain sequences (Figure 17). Murine and bovine β_3 PSI domains either lack a proline or contain two adjacent pralines at position 32 and 33, which differs from Syrian hamster and human β_3 PSI domain and suggest that they are determinants of ANDV binding to β_3 integrins. Previous studies have reported that mutation of the human β3 aspartic acid (N39) to an asparagine in murine β3 was critical for hantavirus susceptibility (86), however, Syrian hamster β3 has an asparagine at this position and this change has no apparent inhibitory effect on Andes virus infection of BHK-21 cells.

Mutation of Human and Bovine PSI Domain

In order to define the role of leucine 33 in ANDV recognition, we mutated the bovine β_3 integrin proline 33 to the leucine (P33L) present in human homologues and then determined whether the bovine P33L PSI domain mutant was capable of inhibiting ANDV infection (Figure 18). We similarly mutated the murine β_3 PSI domain to contain a proline residue at position 32 (S32P) in order to mimic the human β_3 PSI domain. Figure 18 and 19 indicate that the murine β_3 PSI domain fails to inhibit ANDV infectivity while both human and Syrian hamster β_3 PSI domains block ANDV infection. Similar to murine β_3, the WT bovine β_3 PSI domain failed to inhibit ANDV infection of BHK-21 cells and VeroE6 cells (Figure 18). However, the P33L mutant bovine β_3 PSI domain inhibited ANDV infection of VeroE6 and BHK-21 cells by 60% and 55% respectively (Figure 18) and the murine S32P mutant β_3 PSI domain also inhibited ANDV infection of VeroE6 >50% (Figure 19). These finding suggest that the absence of proline 32 or the addition of a second proline at position 32 in the β_3 integrin PSI domain dramatically reduce ANDV recognition of PSI domain polypeptides.

Infection of Recombinant CHO Cells

To further evaluate the effect of P33 on ANDV infection, we reciprocally mutated the full length bovine β_3 subunit to contain P33L and the full length human β_3 to contain L33P. Subsequently we transfected CHO cells with the β_3 mutants and equivalent cell surface expression of human and bovine $\alpha_v\beta_3$ integrins on the surface

of CHO cells was assessed by flow cytometry (Figure 20 and Table 2). CHO cells transfected with human α_v integrin (pcDNA3.1 +/NEO) and either pcDNA4B/ZEO human β_3, human β_3 L33P, bovine β_3 or bovine β_3 P33L integrin were incubated with MAb 1976 (LM609) (Chemicon), an anti-$\alpha_v\beta_3$ antibody directed against a conformational epitope resulting from the post-translational association of the α_v and the β_3 integrin subunits. Equal expression of the $\alpha_v\beta_3$ integrins on the surface of CHO cells was confirmed by flow cytometry (Figure 20).

We determined the susceptibility of CHO cells expressing mutant β_3 subunits to ANDV infection (Figure 21). CHO cells expressing either bovine β_3 or the human β_3 L33P mutant failed to confer ANDV infectivity. In contrast, CHO cells expressing either human $\alpha_v\beta_3$ or a bovine β_3 P33L mutant enhanced ANDV infection >5 fold (Figure 21). These results establish that a proline residue at position 33 inhibits ANDV recognition of β_3 integrin PSI domains and demonstrates sequence specificity for ANDV binding to β_3 integrin.

Chapter 4:

Discussion

Pathogenic hantaviruses are responsible for two severe human diseases, HFRS in Eurasia and HPS in the Americas (94). Both diseases are characterized by acute thrombocytopenia and vascular permeability, which results in hemorrhage in HFRS and acute pulmonary edema in HPS (94, 95). Pathogenic hantaviruses recognize $\alpha_v\beta_3$ integrins expressed on the surface of endothelial cells, the main site of hantavirus replication (26, 29, 86). Endothelial cells line the lumen of capillaries and $\alpha_v\beta_3$ integrins are key regulators of vascular integrity and permeability (128). Interestingly, all pathogenic hantaviruses (HTNV, SNV, PUUV, SEOV, NY-1V, SNV) analyzed thus far use β_3 integrin receptors on human endothelial cells, and cause vascular permeability based diseases, whereas $\alpha_5\beta_1$ integrins are used by nonpathogenic hantaviruses (26, 27, 29, 68).

ANDV Recognizes the PSI Domain of Human and Syrian Hamster β_3 Integrins

ANDV infection of Syrian hamster mimics the long onset, course and symptoms of HPS patients, resulting in a fatal HPS-like disease.

Our results indicate that ANDV infection of either human endothelial cells or Syrian hamster BHK-21 cells was inhibited by the high affinity $\alpha_v\beta_3$ integrin ligand vitronectin. Antibodies against $\alpha_v\beta_3$ integrins and β_3 subunits also inhibited ANDV infection of endothelial cells demonstrating the specificity of ANDV recognition of the human β_3 integrin. Antibodies to human β_3 integrins failed to recognize Syrian hamster β_3 or inhibit ANDV infection of BHK-21 cells. Thus these findings

demonstrate that ANDV infectivity of human endothelial cells is dependent on the presence of β_3 integrins.

Inhibition experiments demonstrated that PSI domain polypeptides derived from either human or Syrian hamster origin, inhibit ANDV infectivity. In contrast, ANDV failed to recognize PSI domain polypeptides of murine or bovine origin. These findings indicate that ANDV selectively recognizes human and Syrian hamster β_3 integrin PSI domains. These findings are consistent with ANDV pathogenesis in both humans and Syrian hamsters.

Small molecule inhibitors and antibodies to β_3 integrin as potential therapeutics

The identification of viral cell surface receptors may spur the development of small molecule inhibitors for preventing hantavirus attachment or entry. Several small molecule inhibitors are already used as antiviral therapy, mainly for HIV (4, 20, 52). Enfuvirtide binds glycoprotein HIV gp41 and blocks HIV cell entry by disturbing the conformational changes in glycoprotein gp41 needed for viral-cell membrane fusion (4). A recent study identified inhibitors of arenavirus infection through high throughput screening of synthetic combinatorial small molecule libraries. The study shows that the small inhibitors of viral entry act at the level of the glycoprotein-mediated membrane fusion with an IC50 = 200-350 nM (59).

A second class of viral entry inhibitors targets the virus itself and these prevent the virus from binding to its receptor (20). An example is DCM205, a small molecule capable of inactivating HIV in vitro by binding to the glycoprotein 120 and disrupting

gp120-CD4 interaction. A third group of antiviral peptides includes compounds that bind to the viral receptors on the cell surface (4, 20, 52). HIV uses CCR5 as co-receptor for cell entry and Maraviroc and Vicriviroc are two compounds that bind CCR5 receptor leaving the receptor unavailable for gp120 interaction (52).

Small molecule therapeutics for hantaviruses disease are non-existent. However, we have shown that two small peptides, β_3 13-49 containing residues 13-49 of the β_3 PSI domain and β_3 17- 48, containing residues 17-48 of the β_3 PSI domain inhibit hantavirus infection of endothelial cells. These findings provide a rationale for developing hantavirus therapeutics using by using β_3 13-49 and β_3 17-48 directly as therapeutic agents or as leads for developing compounds that bind β_3 or mimic the β_3 hantavirus binding site. Other groups have identified inhibitory peptides for SNV, ANDV and HTNV infection of Vero6 cells using phage display libraries (35, 36, 58). Elution of phage using antibodies to $\alpha_v\beta_3$ integrin identified several positive clones which were then used in inhibition assays of SNV and HTNV (58). However, inhibition percentages of the synthesized peptides varied from 51% to 14% but only when applied at a 2 mM concentration. At these peptide levels, it is not clear whether there is any specific inhibitory effect of the peptides. In contrast, our data shows that peptides containing the β_3 integrin PSI domain inhibit hantavirus infection by 75% at 30 μM levels.

A similar approach using commercial antibodies against ANDV Gn and Gc was used to elute phage and identify inhibitory peptides against ANDV (35). The inhibitory peptides showed homology to several β_3 integrin domains of unknown

binding capacity, but none showed homology to the PSI domain (35). The 3 most potent peptides inhibited ANDV infectivity by 57% at a concentration of 1 mM while an internal discrepancy within the paper indicates an IC_{50} of 25-30 μM for each peptide (35).

Antibodies to β_3 integrins such as ReoPro are used clinically to prevent platelet aggregation, clotting and thrombosis following vascular surgery or myocardial infarction or to prevent angiogenesis (Vitaxin) (16). ReoPro is the humanized Fab fragment derived from antibody c7E3 and hantavirus infection is inhibited by c7E3 but not by ReoPro suggesting steric inhibition by c7E3 rather than inhibition by attachment to the hantavirus binding site (26, 35). In fact, mutations at positions 129 and 177-184 of human β3 abolish c7E3 binding and are outside of the PSI domain recognized by pathogenic hantaviruses (16, 26). LM609 is another β3 antibody directed against a conformational epitope formed in the $\alpha_v\beta_3$ heterodimer that inhibits pathogenic hantavirus infection of cells (16, 26).

Due to lack of antibodies to the β_3 integrin PSI domain we developed polyclonal antibodies to the β_3 integrin PSI domain (residues 17-48) and these antibodies inhibit infection by pathogenic hantaviruses NY-1V, HTNV and ANDV. These findings may rationalize the specific development of monoclonal antibodies to human β_3 integrin 17-48 that can be used to block hantavirus infection. However, antibodies to β_3 integrins can have significant side effects and may increase hemorrhagic disease or auto-immune responses to the integrin itself (6, 10, 37).

Development of peptide therapeutics and immunotherapeutics targeting the hantavirus glycoproteins has been limited. Hantaviruses only contain two surface glycoproteins, Gn and Gc, but identification of glycoprotein attachment protein has not been reported (68). GnGc surface proteins are highly insoluble oligomerized heterodimers that are trafficked to the cis-Golgi where hantaviruses bud. Since recombinant GnGc is not trafficked to the plasma membrane, the GnGc domains required for interaction with the β_3 integrin cannot be defined using a cell binding assay (100). Targeted changes in the glycoproteins are prevented by poor expression of Gn and Gc, and their ability to form heterodimers and higher order oligomers. One potential means to circumvent this problem may be to develop a library of overlapping peptides of Gn and Gc surface domains and assay their binding to β_3 integrin PSI domain (residue 17 to 48). Studies have shown that the transfer of neutralizing antibodies from either monkeys or rabbits immunized with an ANDV M (pWRG/AND-M DNA vaccine) protects Syrian hamsters from fatal HPS disease up to five days after ANDV infection (19, 43). These neutralizing antibodies may also target specific GnGc peptides and thereby point to potential peptides that elicit neutralizing antibody responses.

Residue 33 in β_3 Integrin PSI Domain Determines ANDV Recognition.

The species specific use of β_3 integrin PSI domains permitted us to further analyze critical residues within the PSI domain required for ANDV recognition. A comparison of species specific β_3 subunit PSI domains shows that murine and bovine

β_3 sequences either lack a proline residues (murine β_3 integrin) or contain 2 adjacent prolines (bovine β_3 integrin) at positions 32 and 33. Mutagenesis demonstrated that ANDV recognition of human β_3 integrins is abolished by substituting leucine for proline at position 33 of the human β_3 subunit (L33P). Similarly substituting serine for a proline (S32P) in the murine β_3 PSI domain permitted the PSI domain to function as an inhibitor of ANDV infection. Conversely, when proline 33 of the bovine β_3 subunit was replaced by leucine (P33L), the mutant bovine β_3 subunit also conferred cell susceptibility to ANDV infection. These findings indicate that ANDV specificity for β_3 integrins is directed by residues 32 and 33. This differs from recognition sequences of NY-1V and HTNV which appear to be dependent on residues at position 39 and unaltered by residue 32 or 33 substitutions. Previous studies have shown that NY-1V and HTNV required an aspartic acid at position 39 in human β_3 integrin, changing this residue into its murine homologue, an asparagine, abolished NY-1V and HTNV infection of recombinant CHO cells (86). As a result, ANDV recognition of β_3 integrin PSI domains appears to be discrete from other hantavirus binding requirements. However, it is unclear whether β_3 integrin interactions or other changes in these viruses are responsible for the unique ability of ANDV to cause disease in Syrian hamsters. NY-1V is clearly restricted in BHK-21 Syrian hamster cells (Figure 3) and data presented here suggests that this difference may be due to species specific β_3 integrin residues.

The L33P substitution is a naturally occurring β_3 integrin polymorphism which differentiates Human Platelet Antigen 1a (HPA-1a) from HPA-1b. Individuals

positive for HPA-1b allele, heterozygous or homozygous, do not suffer from any obvious health problems, although the polymorphism does modify the function of cells expressing the Pro33 positive β_3 integrin (115, 119, 120). Studies have shown people with the HPA-1b allele have shorter bleeding times and enhanced thrombin generation (119). HPA-1b positive individuals are also at increased risk for myocardial infarction, especially when younger or after revascularization procedures (65). In vitro studies using platelets expressing $\alpha_{IIb}\beta_3$ integrin show increased aggregation, α granule secretion and adhesion (65, 119). In addition, cells expressing Pro33 $\alpha_v\beta_3$ integrin show an enhanced migratory response to vitronectin (119). A possible explanation for these functional differences may be due to a structural change caused by the Leu33Pro substitution.

The PSI domain crystal structure indicates that L33 is located in a flexible loop of the β_3 subunit, and a proline substitution likely has a profound influence on the structure of the β_3 integrin PSI domain (129). The PSI domain plays a role in the conformational switch between an extended and bent integrin and is referred to as the "genu" of the integrin (105). A PSI domain containing proline might be more rigid, which could favor extension of the integrin and keeps the integrin in the active extended form. Such changes would favor ligand binding and outside-in signaling leading to enhance platelet aggregation, cells adhesion, cell spreading and migration (119). Keeping the β_3 integrin in a more activated and thus extended state would also explain why ANDV does not recognize β_3 integrin with a double proline (position 32 and 33). In this case, the PSI domain may not be accessible for ANDV binding.

However, polypeptides expressing bovine β_3 integrin PSI domains as well as human PSI domain mutants containing L33P substitutions are also unable to inhibit ANDV infection and demonstrate that the L33P change by itself determines ANDV recognition.

Interestingly, the L33P substitution is also sufficient to direct autoimmune responses to β_3 integrins from blood containing a different HPA type and this immune response to β_3 results in two auto-immune diseases, Fetomaternal Allo-immune Thrombocytopenia (FMAIT) and Post Transfusion Purpura (PTP) (49, 51). FMAIT and PTP patients display vascular permeability and acute thrombocytopenia similar to symptoms of hantavirus infected HFRS and HPS patients hantavirus (47, 49). In fact, it is possible that hantavirus interactions with inactive β_3 integrins could result in antibody responses against platelet β_3 integrin receptors or hantavirus-β_3 integrin complexes and similar to drug-induced thrombocytopenia, contribute to thrombocytopenia and permeability deficits within hantavirus patients. ANDV infection of endothelial cells is blocked by the presence of a proline at residue 33 of the β_3 integrin subunit. This suggests that the L33P polymorphism could be a determinant of patient susceptibility to pathogenic hantaviruses. Our results permit us to hypothesize that individuals homozygous for HPA-1a (L33) could be more susceptible to ANDV infection and disease than individuals homozygous for HPA-1b (P33). One study has indicated that a polymorphism in the HPA-3b allele (I843S) of $\alpha_{IIb}\beta_3$ integrins results in more severe clinical HFRS disease (63). Although, the findings did not address a significant difference in HFRS disease severity in HPA-1

genotype distributions. Only 1% of Asian patients are homozygous for the HPA-1b allele and thus the study could not determine whether HPA-1b reduced hantavirus disease (103). Further information on the role of HPA-1 polymorphisms in hantavirus infection have not been defined but since only 1-15% of specific populations are homozygous for HPA-1b, testing will require a large number of hantavirus patients. Similar experiments to test this hypothesis could also be accomplished by comparing ANDV infection of endothelial cells derived from HPA-1a and HPA-1b patients.

Hantavirus Pathogenesis

There is no patient data indicating that β_3 integrins are the cause of vascular permeability in hantavirus diseases. However, β_3 integrins on platelets and endothelial cells have primary roles in regulating vascular integrity and pathogenic hantaviruses clearly alter the permeability of infected endothelial cells in a manner consistent with the effects of β_3 integrin dysregulation (16, 26-29, 68, 86, 88, 89). Pathogenic hantaviruses selectively inhibit β_3 integrin directed migration and enhance endothelial cell permeability in response to VEGF. Hantavirus regulation of endothelial cell integrin functions is not the result of virus adsorption, since low MOIs (0.1-1) are applied to cells and neither endothelial cell migration nor endothelial cell permeability are altered at early times after infection (27, 28, 86). Inhibited migration and enhanced permeability of endothelial cells is only observed days after infection when hantaviruses reportedly coat the surface of infected endothelial cells (27, 28, 34). In fact pathogenic hantaviruses may remain cell associated through hantavirus-β_3

interactions on the surface of endothelial cells, and thus contribute to β_3 dysfunction and enhanced endothelial cell permeability days after viral emergence.

Thrombocytopenia is another hallmark of patients infected by pathogenic hantaviruses (18, 94, 131). However, neither the role of platelets in hantavirus disease nor the mechanism of hantavirus induced thrombocytopenia has been defined. Cosgriff et al. demonstrated that platelets from HFRS patients are defective in platelet function (aggregation and granule release) and that this defect was not the result of a soluble circulating factor. This implies that thrombocytopenia in HFRS patients results from a block in platelet activation, rather than from excessive platelet activation (17). This platelet defect following hantavirus infection, together with an understanding of hantavirus binding to inactive β_3 integrins, suggests that hantaviruses may bind inactive $\alpha_{IIb}\beta_3$ integrin conformers and prevent platelet activation. Since hantaviruses are largely cell associated at late times after infection (34) this also suggests that cell surface displayed hantaviruses could potentially recruit quiescent platelets to the endothelial cell surface and simultaneously prevent platelet activation, reduce the level of activated platelets and mask the presence of hantavirus infected cells.

Our findings do not exclude additional immunologic mechanisms which may contribute to hantavirus pathogenesis and vascular permeability (38, 53, 54, 62, 72, 104, 108, 109). Immune complex deposition clearly contributes to HFRS patient disease and the development of renal sequelae. According to Cosgriff, hantavirus infection in HFRS patients leads to formation of immune complexes which may

activate platelets. Activated platelets circulate in the bloodstream but remain in the circulating platelet pool. These circulating platelets demonstrate impaired aggregation and release responses (17). Other immunologic mechanisms include $CD8^+$ cells, TNFα and viremia.

a) *$CD8^+$ cells*: A higher frequency of $CD8^+$ T-cell responses was stated to cause more severe HPS. However, the data demonstrates that there are little or no differences in SNV specific T-cell responses in HPS patients with severe or moderate disease. In fact, fatal outcome patients had a similar $CD8^+$ T-cell response compared to those with moderate disease (54). Researchers also reported that a $CD8^+$ SNV specific T lymphocyte cell line, which recognized and lysed human endothelial cells, caused increased permeability (38). However, controls are lacking in many of these experiments and the peptide specific activation of T-cells was not demonstrated within this report. In fact the endothelial cell lysis reported does not reflect patient or in vitro findings where the lysis of endothelial cells is not observed (94).

b) *TNFα*: Several studies have evaluated the effect of TNFα in hantavirus infected patients and endothelial cells (17, 53, 55, 62, 75, 109). One study concludes that elevated TNFα, IL-1 and IL-6 do not correlate with HFRS disease as only 5% of HFRS sera had elevated cytokines (55). In another study, elevated TNFα was seen in 15 HFRS sera however, these sera also presented a high level of TNFRs which bind TNFα and prevent cellular responses to TNFα (62). Increased TNFα was observed in the glomeruli of HFRS patients (109), which is

also the site where immune complexes are observed (17), however, other studies showed that low levels of TNFα are associated with severe HFRS disease and linked to decreased hantavirus clearance (70). In support of reduced pathogenesis caused by TNFα induction, a recent report indicates that a 40 fold induction of TNFα in alveolar fluid was associated with a 90% reduction in lethal influenza virus infection rather than increased pulmonary disease (114). HPS pathogenesis has also been associated with high levels of cytokine producing cells in the lung tissues of two of six fatal HPS cases (72). However, the four other cases showed a low level of TNFα in their lung tissue, and one case actually showed no TNFα positive cells (72). Two studies also evaluated TNFα directed permeability of endothelial cells. The first paper states that TNFα caused prolonged hyperpermeability of HTNV infected endothelial cells yet only one TNFα induced permeability finding was presented (< 2 fold increase) (75). The second study found no association between TNFα induced permeability and SNV infected endothelial cells (53). This study is also consistent with a recent paper stating that the N-protein of HTNV regulates TNFα directed cellular responses (108).

c) *Viremia*: Hantavirus viremia is associated with increased pathogenesis in human and Syrian hamsters (13, 109, 110). Although is unclear what role viremia plays in hantavirus pathogenesis, increased viremia provides a means for circulating hantaviruses to interact with β_3 integrins, on platelets, endothelial cells and immune cells throughout the body. Viremia could result in defective platelet

aggregation which is already reported for HFRS patients (17) suggesting that the platelet dysfunction rather than activation contributes to hantavirus pathogenesis.

Potential Mechanism of Vascular Mechanism in Hantavirus Disease

The mechanism of hantavirus induced vascular permeability has yet to be defined. Our results show that there is clear role for β_3 integrin dysfunction in vascular permeability deficits which makes hantavirus interaction with β_3 integrin subunits important for cell disease processes. Pathogenic hantaviruses enhance endothelial cell permeability in response to VEGF (27) suggesting that pathogenic hantaviruses disrupt endothelial cell adhesion. Endothelial cell barrier functions are mainly provided by adherens junctions, which are composed of the endothelial cell specific protein, vascular endothelial (VE)-cadherin (56, 57). Genetic deletion of VE-cadherin or mutations decrease VE-cadherin binding and result in increased capillary permeability (25). VEGFR2 activation directs VE-cadherin phosphorylation, dissociation and internalization and increases endothelial permeability by directing the disassembly of adherens junctions (24, 122, 132). $\alpha_v\beta_3$ integrins interact with the vascular endothelial growth factor receptor 2 (VEGFR2) and thus have a primary role in regulating vascular permeability (11, 42, 87, 89). Pathogenic hantavirus interactions with inactive $\alpha_v\beta_3$ may disrupt normal β_3-VEGFR2 interaction and thereby increase permeabilizing responses to VEGF that cause the internalization of VE-cadherin and intercellular permeability. A potential model for this mechanism is shown in Figure 22. Endothelial cell adherence junctions, which regulate vascular

permeability, may be dissociated as a result of pathogenic hantavirus interactions with β_3 integrins and result in enhanced vascular permeability. As a result, hantavirus interactions with inactive $\alpha_v\beta_3$ provides a means for cell surface associated hantaviruses to alter VEGF responses and endothelial cell permeability.

Thrombocytopenia is another hallmark of patients infected by pathogenic hantaviruses (76, 94, 131). However, neither the role of platelets in hantavirus disease nor the mechanism of hantavirus induced thrombocytopenia has been defined. Thrombocytopenia in HFRS patients results from a block in platelet activation (17) and is consistent with hantavirus binding to inactive$\alpha_{IIb}\beta_3$ integrins. This suggest that hantaviruses may bind inactive $\alpha_{IIb}\beta_3$ integrins on platlets and regulate platelets activation. However, this also suggests that platelets are likely to transport hantaviruses throughout the vasculature, potentially mask hantaviruses and if hantaviruses enter platelets they could even serve as a site for hantavirus replication. Since SNV was reported to be largely cell associated at late times after infection (34), this also suggests that cell surface displayed hantaviruses could potentially recruit quiescent platelets to the endothelial cell surface. Recruited quiescent platelets may form a platelet layer which covers the surface of infected endothelial cells (Figure 23) and simultaneously prevents platelet activation, reduce the level of activated platelets and masks the presence of hantavirus infected cells.

The role of platelets in carrying hantaviruses throughout the vasculature and adhering to the endothelium are of fundamental importance since both are linked to the regulation of vascular integrity and platelet deposition could cause localized

hypoxia. Hypoxic conditions enhance the stability of a Hypoxia Induced factor 1a (HIF-1 α) complex which transcriptionally induces VEGF. In turn, VEGF enhances the stability of HIF-1α, further activating hypoxic response and forming a hypoxia-VEGF autocrine loop (106). This may be especially significant in narrow microvascular pulmonary alveolar beds where gas exchanges occur (101). As a result, studies of hantavirus interaction with platelets will provide insight into the role of platelets in the hantavirus life cycle and contribute to an understanding of why hantaviruses cause thrombocytopenia.

Chapter 5

Figures and Legends

HANTAVIRUS	HOST	LOCATION	DISEASE
Hantaan Virus (HTNV)	*Apodemus agrarius*	Asia, Far East Russia	HFRS
Dobrava (DOBV)	*Apodemus agrarius* *Apodemus flavicollis*	Balkans, Europe	HFRS
Seoul (SEOV)	*Rattus norvegicus*	Worldwide	HFRS
	Rattus rattus		
Puumala (PUUV)	*Clethrionomys glareolus*	Europe	HFRS
New York -1 (NY-1V)	*Peromyscus leucopus*	Eastern US	HPS
Sin Nombre Virus (SNV)	*Peromyscus maniculatus*	West and Central US, Canada	HPS
Bayou Virus (BAYV)	*Oryzomys palustris*	Southeastern US	HPS
Black Creek Canal Virus (BCCV)	*Sigmodon hispidus*	Florida (US)	HPS
Andes virus (ANDV)	*Oligoryszomys longicaudatus*	Argentina and Chili	HPS
Oran Virus	*Oligoryszomys longicaudatus*	Northwestern Argentina	HPS
Prospect Hill Virus (PHV)	*Microtus pennsylvanicus*	US	None
Tula virus (TULV)	*Microtus arvalis* *Microtus rossiaemeridionalis*	Europe	None

Table 1: Hantaviruses, hosts, location and associated disease (modified from cdc.gov)

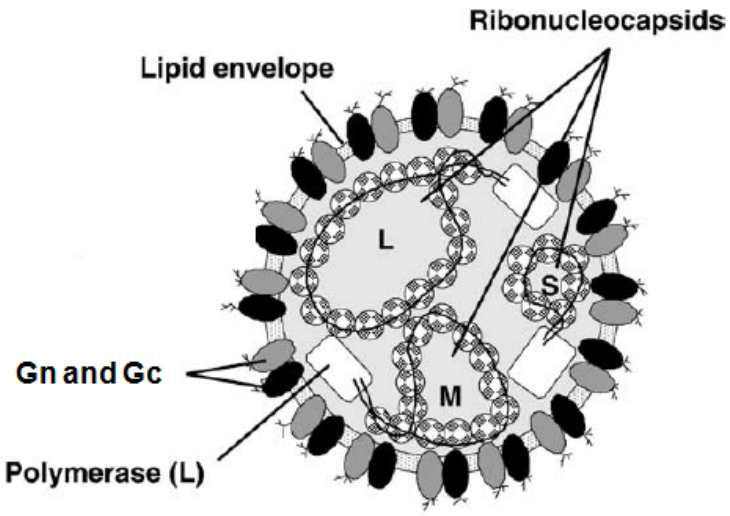

Figure 1 Representation of the hantavirus and encoded proteins (127)**.** Hantaviruses are spherical enveloped viruses with a tri-segmented negative-sensed RNA genome: Small (S) segment encodes the ribonucleocapsid, Medium (M) segment encodes viral glycoprotein Gn and Gc expressed at the viral surface and the large (L) encodes the RNA dependent RNA polymerase (RdRp).

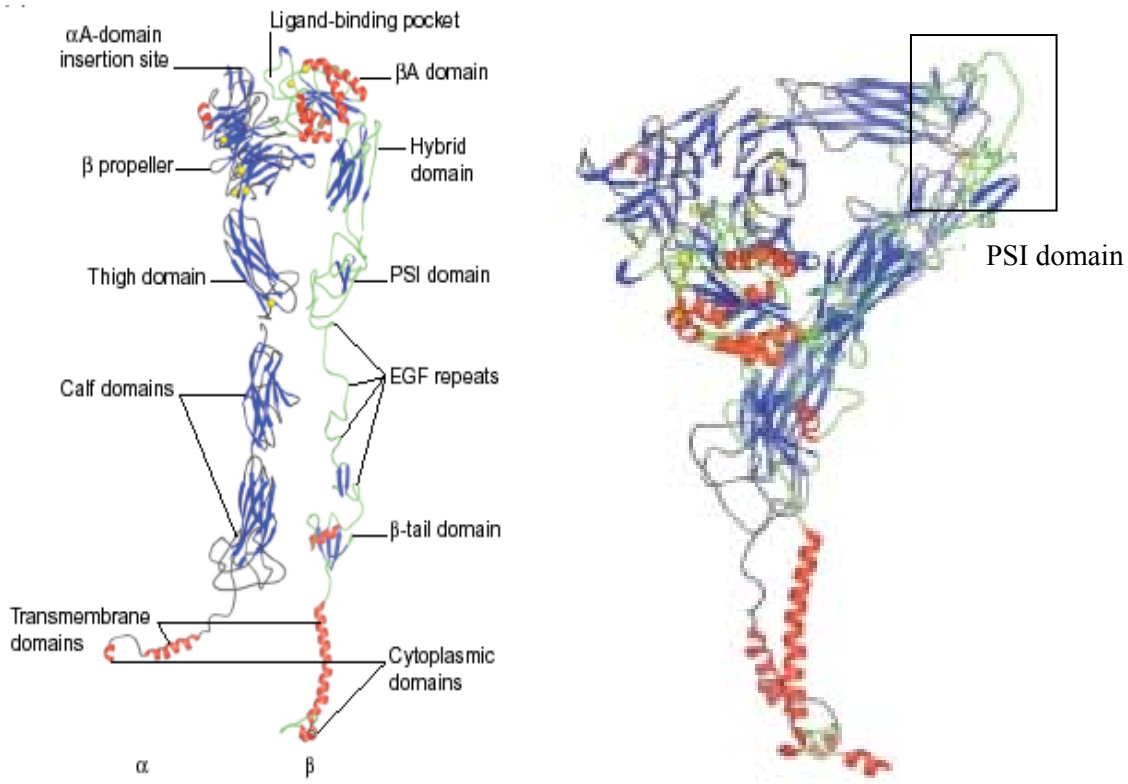

Figure 2 Schematic representation of extended (A) and bent (B) αvβ3 integrin (Pictures derived from reference 45). The α subunit comprises a β propeller at the top, followed by three sandwich modules (thigh and calf domains), a transmembrane domain and a short cytoplasmic tail. The β subunit comprises an A domain , followed by a β-sandwich hybrid domain four epidermal growth factor (EGF) repeats and a β tail domain (45). The PSI domain, located at the apex of the bent integrin (B), is boxed.

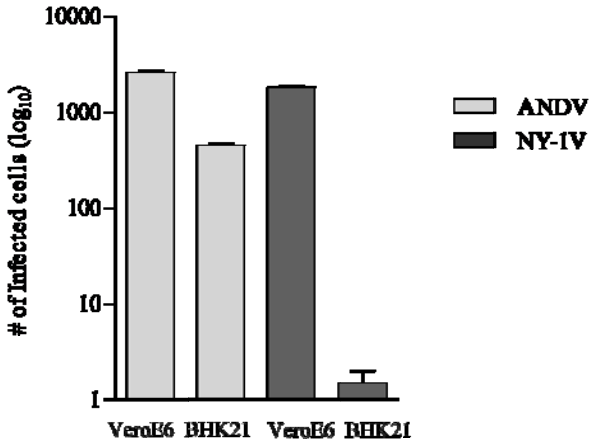

Figure 3 Replication of ANDV and NY-1V in VeroE6 cells and BHK-21 cells. BHK-21 cells and VeroE6 cells were identically infected with ANDV and NY-1V at an MOI of 0.5. The number of hantavirus infected cells was quantitated 3 days post infection by immunoperoxidase staining of the viral nucleocapsid protein.

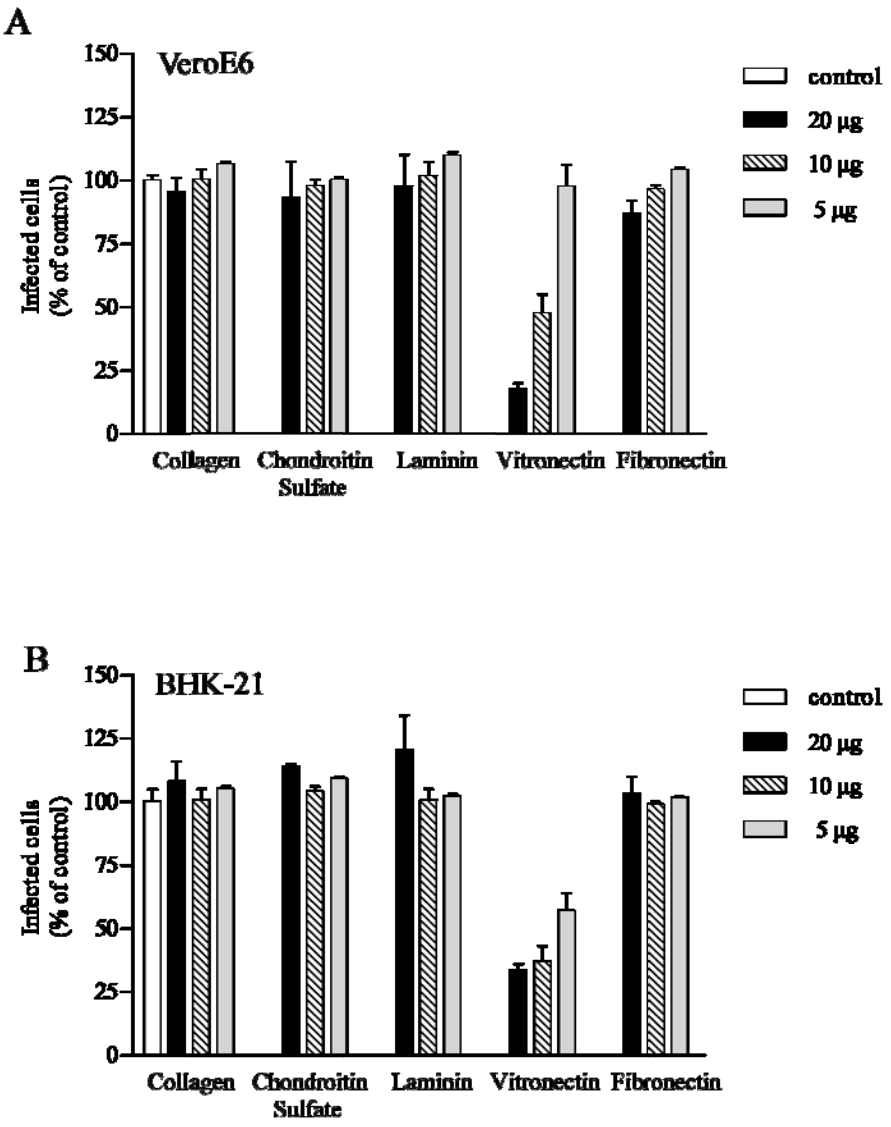

Figure 4 Ligand-specific Inhibition of ANDV Infection. Potentially competitive ligands (5-20 µg/ml) were adsorbed to VeroE6 **(A)** and Syrian hamster BHK-21 **(B)** cells for 1 hour at 4° C prior to virus addition. Approximately 1000 FFUs of ANDV were adsorbed for 1 hour at 37° C to duplicate wells of a 96-well plate. Following viral adsorption, inocula were removed and cells were washed and incubated 24 hours at 37° C before methanol fixation. ANDV infected cells were identified by immunoperoxidase staining of the viral nucleocapsid protein and quantitated by microscopy as previously described (86). Results were reproduced in at least two separate experiments and presented as a percent of controls.

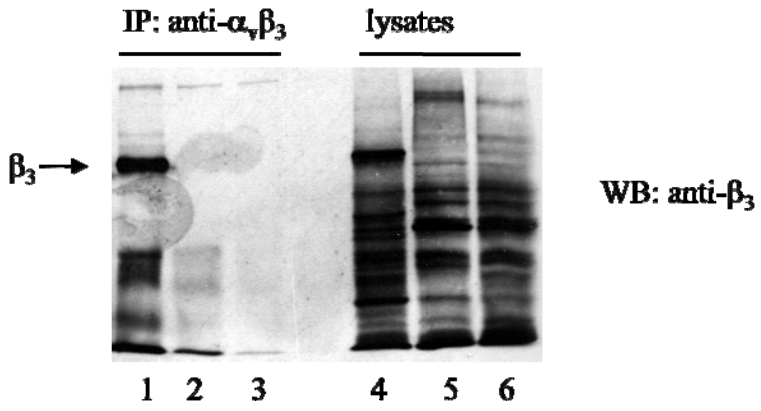

Figure 5 Antibodies to human $\alpha_v\beta_3$ Integrins and β_3 Integrins do not Recognize Syrian hamster β_3 Integrins. VeroE6 (lane 1), CHO (lane 2) and BHK-21 (lane 3) cell lysates were incubated with monoclonal anti-$\alpha_v\beta_3$ integrin for β_3 immunoprecipitation and immunocomplexes were isolated on protein A/G agarose beads. 10 µl of the immunoprecipitate and 10 µg of the VeroE6 (lane 4), CHO (lane 5) and BHK-21 (lane 6) cell lysates was loaded on a 7% SDS-PAGE gel. Immunoprecipitated β_3 integrins and β_3 integrins were detected using polyclonal anti-β_3 integrin. IP: Immunoprecipation, WB: Western blotting.

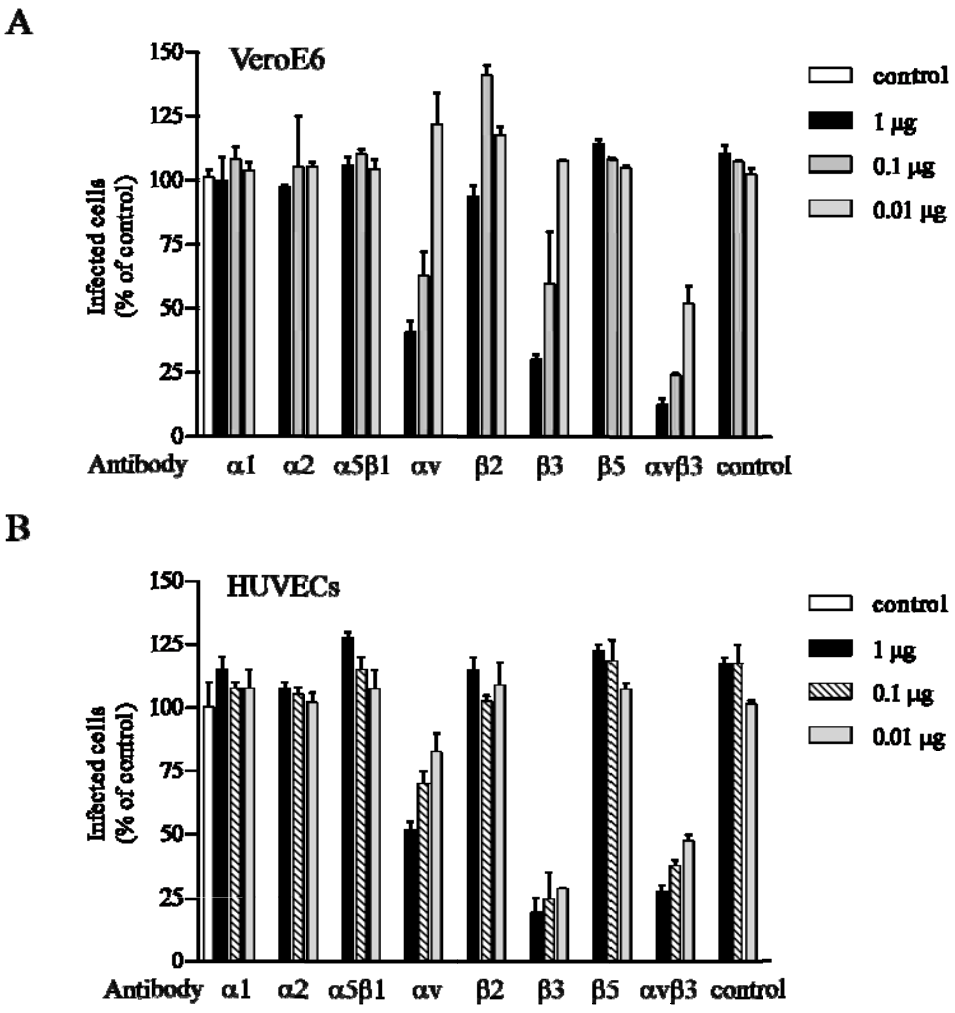

Figure 6 ANDV Infectivity is Inhibited by Integrin-specific Antibodies.
Duplicate wells with VeroE6 cells **(A)** and HUVECs **(B)** were pretreated for 1 hour at 4° C with 0.01-1 µg of antibodies to indicated integrins or integrin subunits prior to viral adsorption. Monolayers were washed with PBS and ~1000 FFUs of ANDV was adsorbed to cells for 1 hour at 37° C. Inocula were removed and the number of ANDV infected cells was quantitated as previously described (29). Results were reproduced in at least two separate experiments and presented as a percent of controls.

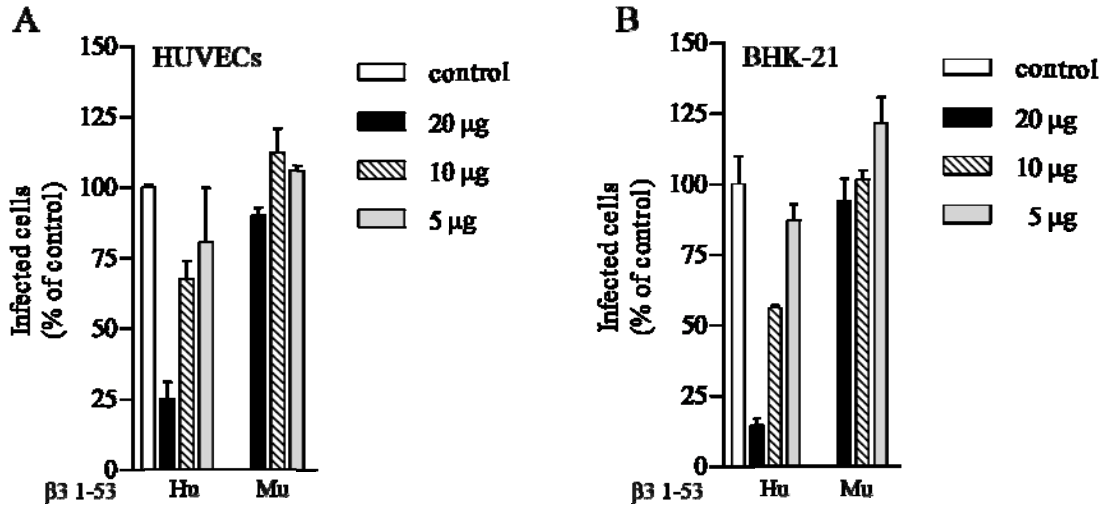

Figure 7 Human β_3 Integrin PSI Domain Polypeptides Inhibit ANDV Infection. Increasing amounts (5-20 μg) of expressed and purified polypeptides containing residues 1-53 of human (Hu) or murine (Mu) β_3 integrins were incubated for 2 hours at 4° C with ~1000 FFUs of ANDV. Virus was subsequently adsorbed to HUVECs **(A)** or BHK-21 cells **(B)** in 96-well plates for 1 hour at 37° C. Monolayers were washed with PBS and 1 day post-infection the number of ANDV infected cells was quantitated after methanol fixation and immunoperoxidase staining of the hantavirus nucleocapsid protein as previously described (86). Results were reproduced in at least two separate experiments and presented as a percent of mock treated controls.

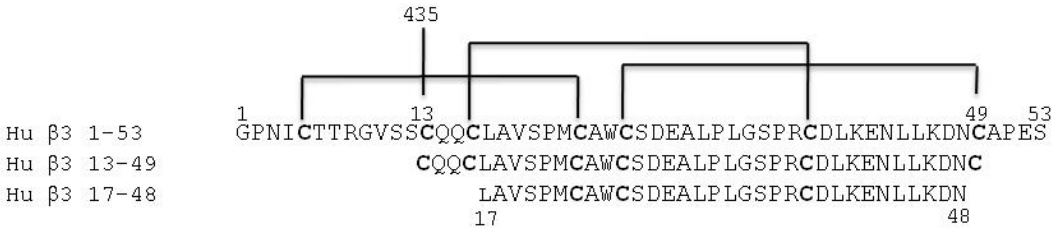

Figure 8 Design of Synthetic Peptides β_3 13-49 and 17-48 based on Conserved Cysteines. Residue 1-53 from human subunits β_3 integrin is presented. Peptide 1-53 contains 7 cysteine residues but Cys13 forms a long range disulfide bond with Cys435. 3 paired cysteine residues, 5-23, 16-38 and 26-49 are present in the β3 integrin PSI domain (1-53). Peptide β3 13-49 contains two disulfide bonds, 16-38 and 26-49, all native intramolecular disulfide bonds are eliminated in β_3 17-48 peptide. Disulfide bonds are indicated by lines.

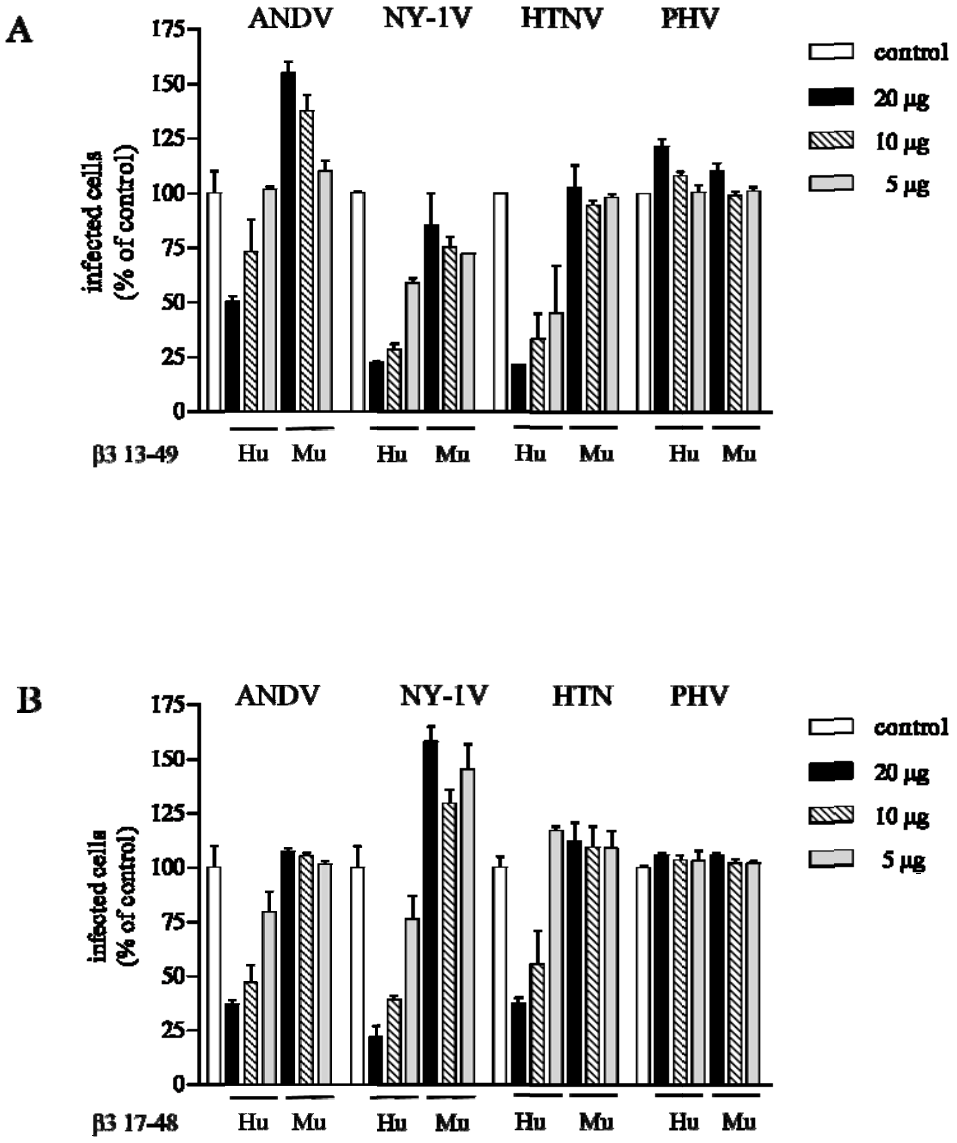

Figure 9 Human β_3 Integrin PSI Domain Polypeptides 13-49 and 17-48 Inhibit ANDV, NY-1V and HTNV Infection. Increasing amounts (5-20 µg) of expressed and purified polypeptides containing residues 13-49 **(A)** and 17-48 **(B)** of human or murine β_3 integrins were incubated for 2 hours at 4° C with ~1000 FFUs of ANDV, NY-1V, HTNV and PHV. Virus was subsequently adsorbed to VeroE6 cells in 96-well plates for 1 hour at 37° C. Monolayers were washed with PBS and 1 day post-infection the number of hantavirus infected cells was quantitated after methanol fixation and immunoperoxidase staining of the hantavirus nucleocapsid protein as previously described (86). Results were reproduced in at least two separate experiments and presented as a percent of mock treated controls.

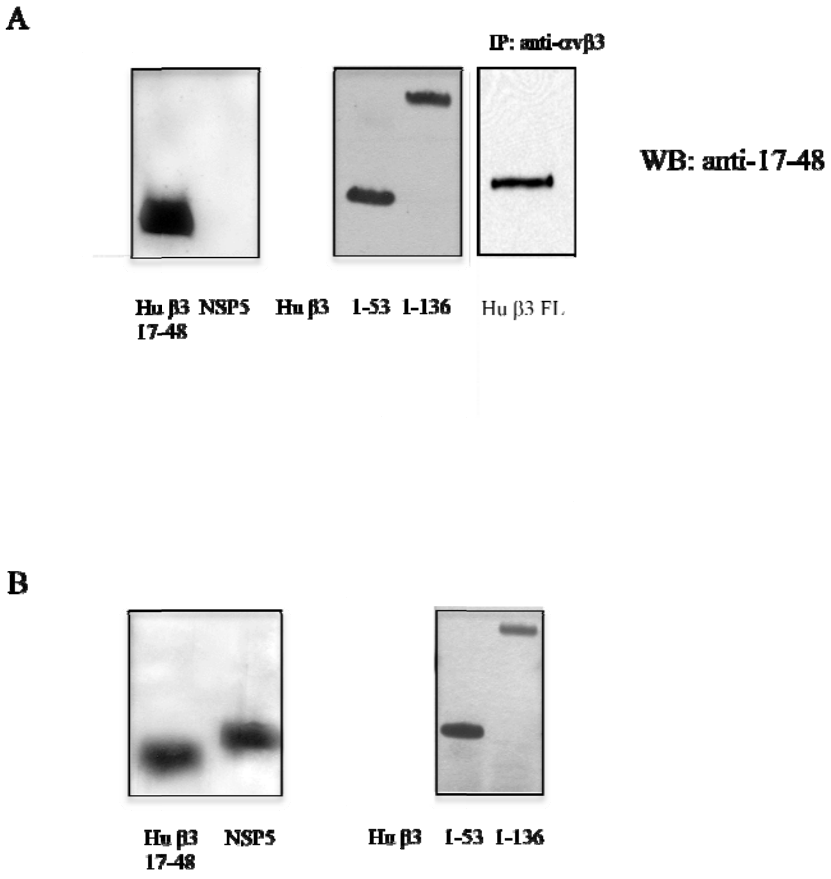

Figure 10 Antibodies to human β_3 Integrin PSI domain (residues 17-48) specifically react with β_3 polypeptide residues 1-53 and 1-136 and full length β_3 Integrin. 1 μg of synthetic peptide 17-48 and purified β_3 1-53 and 1-136 polypeptides were loaded on a 15% SDS-PAGE gel. Full length β_3 integrin was immunoprecipitated from VeroE6 cells using monoclonal anti-$\alpha_v\beta_3$ integrin. 10 μl of the immunoprecipitate was loaded on a 7% SDS-PAGE gel. Proteins were transferred to a nitrocellulose blot and stained with polyclonal anti-β_3 17-48. Rotavirus synthetic polypeptide of NSP5 was used as a negative control **(A)**. Silver staining of loaded polypeptides is shown on bottom panel **(B)**. IP: Immunoprecipation, WB: Western blotting.

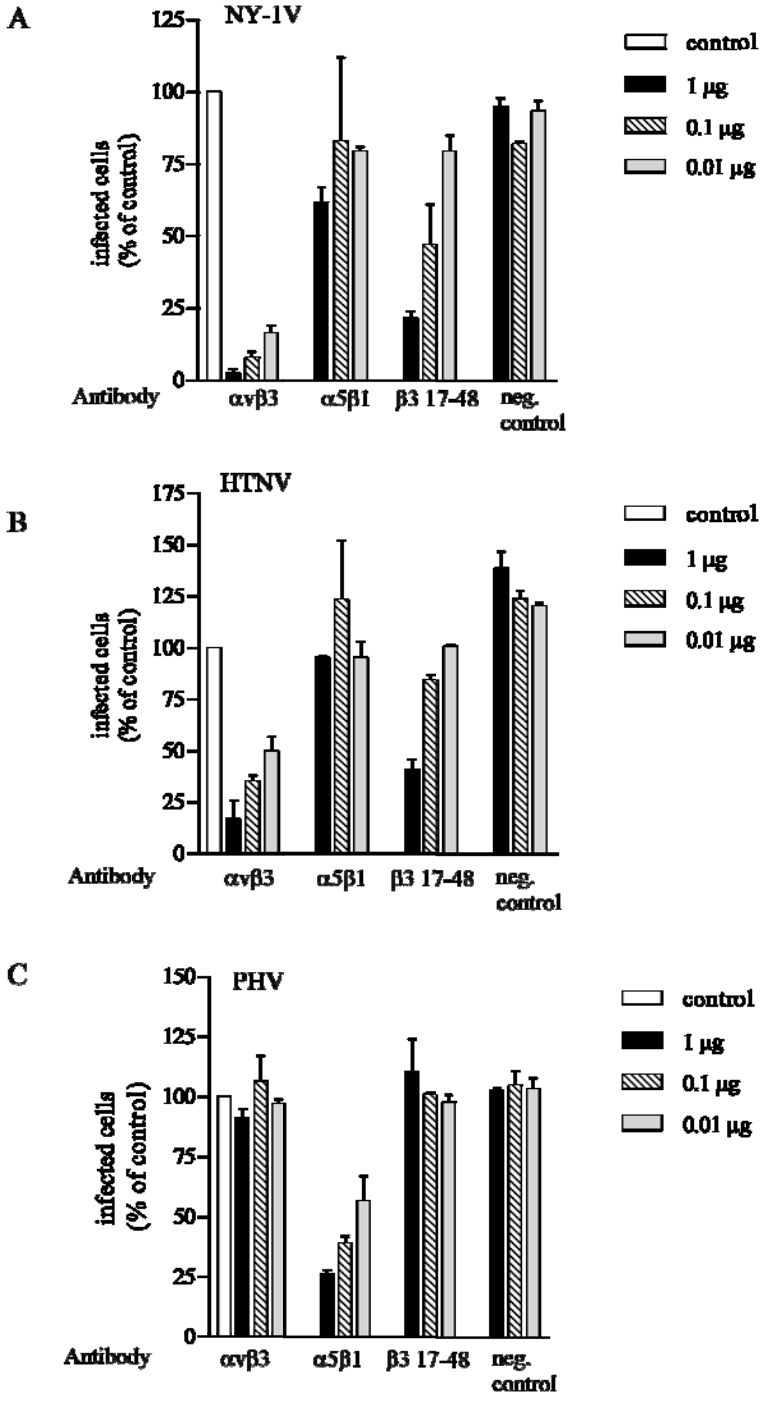
A
NY-1V
125
100
75
50
25
0
infected cells (% of control)
Antibody
αvβ3
α5β1
β3 17-48
neg. control
control
1 µg
0.1 µg
0.01 µg
B
HTNV
175
150
125
100
75
50
25
0
infected cells (% of control)
Antibody
αvβ3
α5β1
β3 17-48
neg. control
control
1 µg
0.1 µg
0.01 µg
C
PHV
150
125
100
75
50
25
0
infected cells (% of control)
Antibody
αvβ3
α5β1
β3 17-48
neg. control
control
1 µg
0.1 µg
0.01 µg

Figure 11

Figure 11 Antibodies to Human β_3 Integrin PSI domain Inhibit NY-1 and HTNV Infection. Duplicate wells of VeroE6 cells **(A)** were pretreated for 1 hour at 4° C with 0.01-1 μg of pre-immune antibody or rabbit antibodies generated to a peptide containing residues 17-48 of the human β_3 integrin PSI domain. Subsequently cells were washed with PBS and ~1000 FFUs of NY-1V, HTNV and PHV were adsorbed to monolayers in duplicate wells of a 96-well plate for 1 hour at 37° C. Following viral adsorption, inocula were removed and cells were washed and incubated 24 hours at 37° C before methanol fixation. The number of NY-1V, HTNV and PHV infected cells were quantitated by immunoperoxidase staining of the hantavirus nucleocapsid protein as previously described (29). Results were reproduced in two separate experiments and presented as a percent of untreated controls.

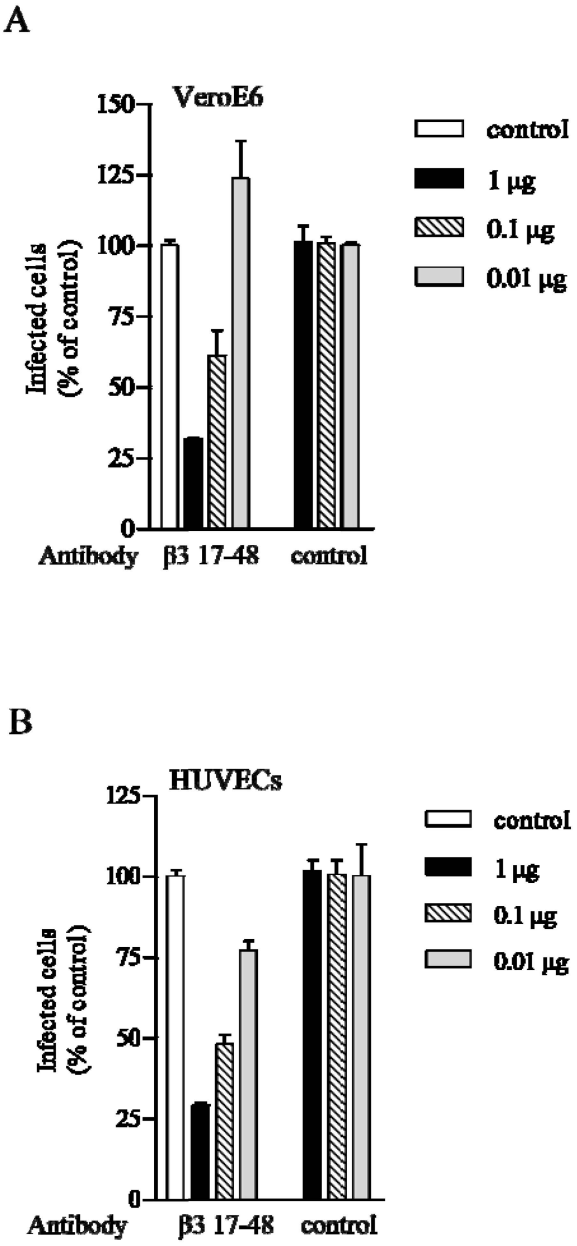
A
VeroE6
150
125
100
75
50
25
0
Infected cells
(% of control)
control
1 µg
0.1 µg
0.01 µg
Antibody
β3 17-48
control
B
HUVECs
125
100
75
50
25
0
Infected cells
(% of control)
control
1 µg
0.1 µg
0.01 µg
Antibody
β3 17-48
control

Figure 12

Figure 12 Antibodies to Human β_3 Integrin PSI domain Inhibit ANDV Infection. Duplicate wells of VeroE6 cells **(A)** or HUVECs **(B)** were pretreated for 1 hour at 4° C with 0.01-1 μg of preimmune antibody or rabbit antibodies generated to a peptide containing residues 17-48 of the human β_3 integrin PSI domain. Subsequently cells were washed with PBS and ~1000 FFUs of ANDV were adsorbed to monolayers in duplicate wells of a 96-well plate for 1 hour at 37° C. Following viral adsorption, inocula were removed and cells were washed and incubated 24 hours at 37° C before methanol fixation. The number ANDV infected cells were quantitated by immunoperoxidase staining of the hantavirus nucleocapsid protein as previously described (29). Results were reproduced in two separate experiments and presented as a percent of untreated controls.

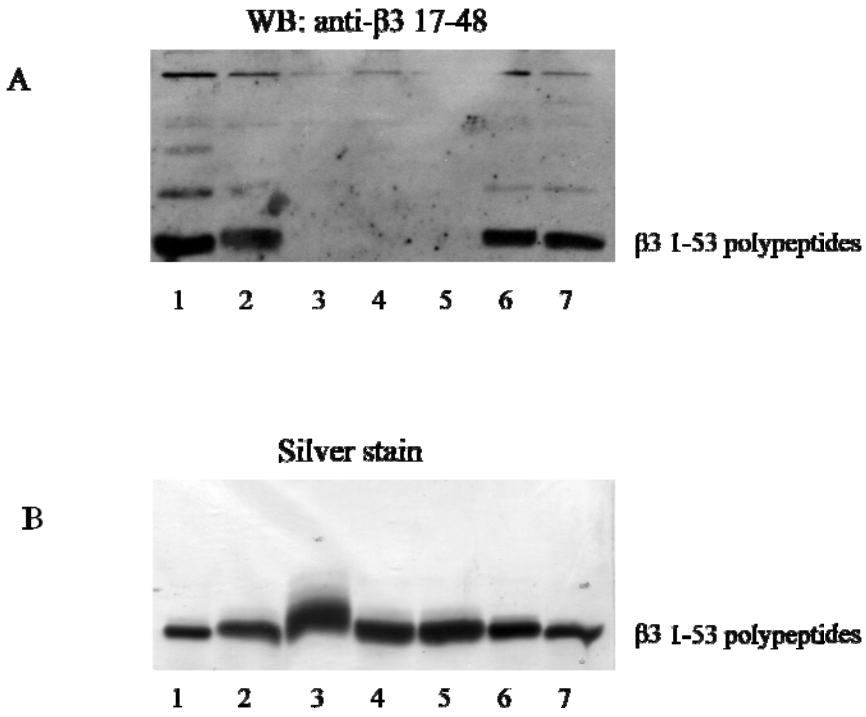

Figure 13 Antibodies to human β_3 PSI Domain (residues 17-48) does not Recognize Syrian hamster β_3 PSI Domain. 2 μg of purified human, murine, Syrian hamster N39, Syrian hamster and bovine β_3 1-53 polypeptides were loaded on a 15% SDS-PAGE gel. Proteins were transferred on a nitrocellulose blot and stained with polyclonal anti-β_3 17-48. Lane 1: human β_3 1-53; lane 2: murine β_3 1-53; lane 3: Syrian hamster β_3 1-53 D39 ; lane 4: Syrian hamster β_3 1-53 N39; lane 5: Syrian hamster β_3 1-53 N39 Q33P; lane 6: bovine β_3 1-53; Lane 7: bovine β_3 1-53 P33L **(A)**. Silver staining of loaded polypeptides is shown on bottom panel **(B)**.

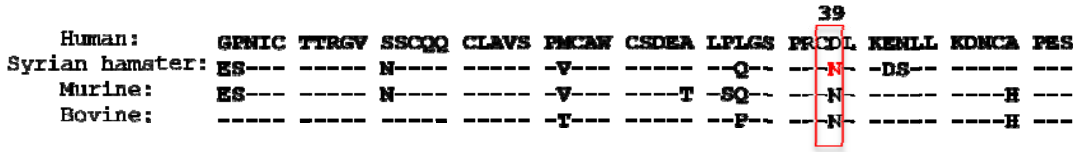

Figure 14 Alignment of Human, Syrian hamster, Murine and Bovine β_3 Integrin PSI Domains. Amino acid sequences of residue 1-53 from human, Syrian hamster, murine and bovine β_3 integrin (GenBank accession number: NM_00012 (human), NM_016780 (murine) and XM_616376, (bovine)) subunits are comparatively presented. Residue differences observed in β_3 integrin homologues which differ from human β_3 sequences are indicated and dashes indicate identical residues. Residue differences at position 39 of β_3 integrin homologues are boxed.

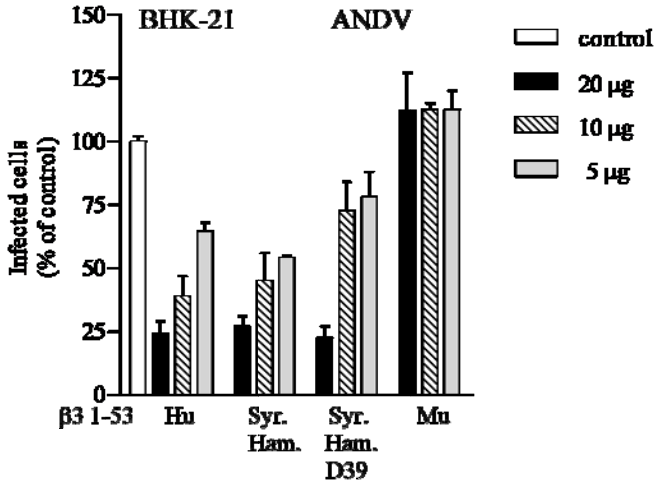

Figure 15 Human β_3 and Syrian hamster β_3 Integrin PSI Domain Inhibit ANDV Infection of BHK21 cells. Increasing amounts (5-20 μg) of expressed human β_3 (Hu), Syrian hamster β_3 (Syr. Ham.), Syrian hamster β_3 D39 (Syr. Ham. D39) and murine β_3 (Mu) β_3 integrin PSI domain polypeptides were incubated with ~1000 FFUs of ANDV for 2 hours at 4° C. Virus was subsequently adsorbed to VeroE6 cells, BHK-21 cells or HUVECs in a 96-well plate for 1 hour at 37° C. Twenty four hours post-infection monolayers were immunoperoxidase stained for the nucleocapsid protein as previously described (86).

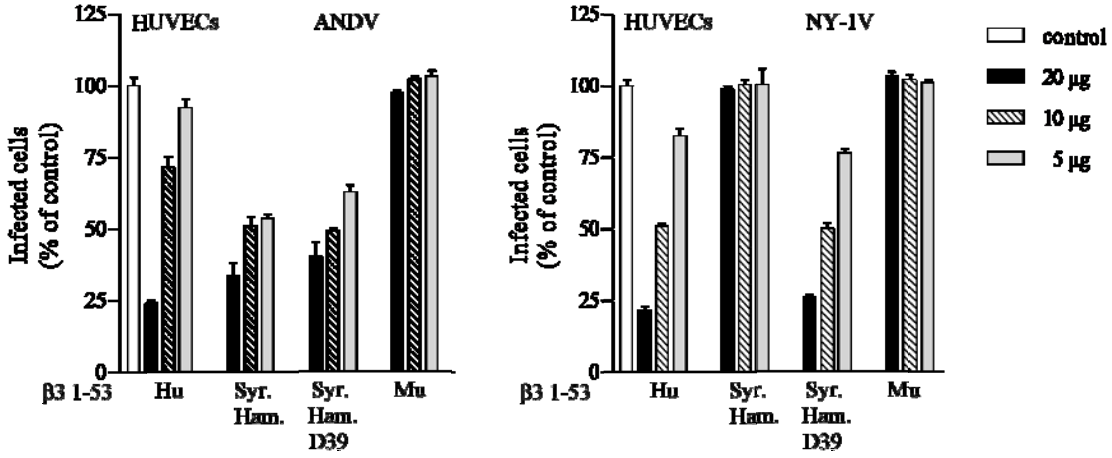

Figure 16 Syrian hamster β_3 N39 Integrin PSI Domain Inhibits ANDV but not NY-1V Infection of HUVECs. Increasing amounts (5-20 µg) of expressed human β_3 (Hu), Syrian hamster β_3 (Syr. Ham.), Syrian hamster β_3 D39 (Syr. Ham. D39) and murine β_3 (Mu) integrin PSI domain polypeptides were incubated with ~1000 FFUs of ANDV and NY-1V for 2 hours at 4° C. Virus was subsequently adsorbed to HUVECs in a 96-well plate for 1 hour at 37° C. Twenty four hours post-infection monolayers were immunoperoxidase stained for the nucleocapsid protein as previously described (86). Results were reproduced in at least two separate experiments and presented as a percent of mock treated controls.

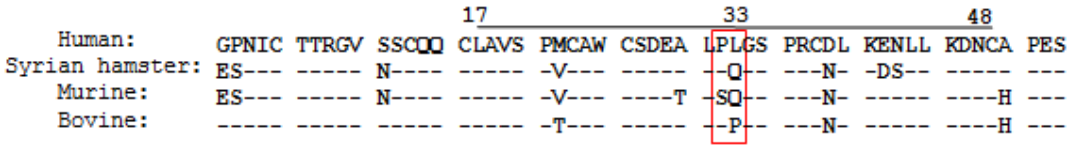

Figure 17 Residues 32 and 33 in human and Syrian hamster β_3 Integrin PSI Domains are discrete from murine and Bovine β_3 Integrin PSI Domains Amino acid sequences of residue 1-53 from human, Syrian hamster, murine and bovine β_3 integrin (GenBank accession number: NM_00012 (human), NM_016780 (murine) and XM_616376, (bovine)) subunits are comparatively presented. Residue differences observed in β_3 integrin homologues which differ from human β_3 sequences are indicated and dashes indicate identical residues. Residue 17 to 48 are delineated by a line and residue differences at positions 32 and 33 of β_3 integrin homologues are boxed.

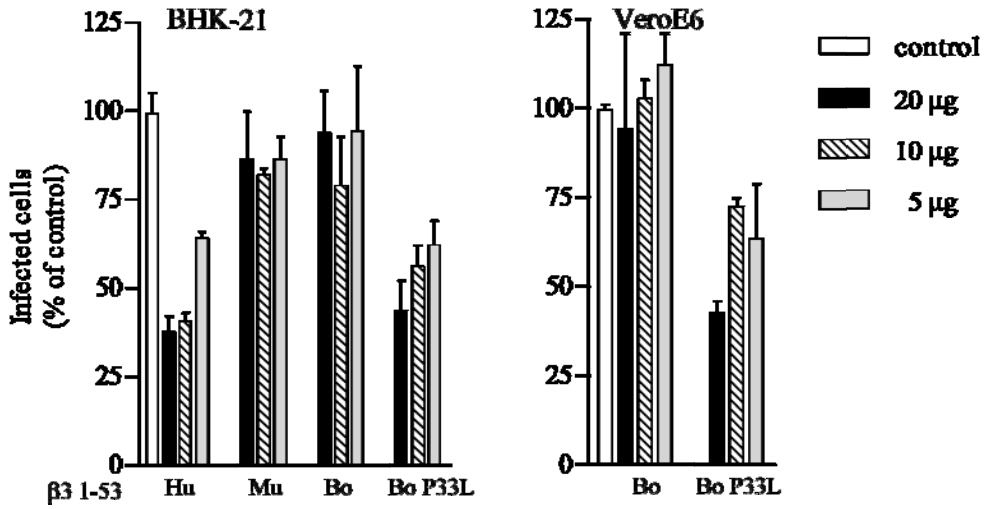

Figure 18 P33L Mutants of the Bovine β_3 Integrin Inhibit ANDV Infection. Increasing amounts (5-20 µg) of human (Hu), murine (Mu), bovine (Bo) wt or bovine P33L (BoP33L) β_3 integrin PSI domain were incubated with ~1000 FFUs of ANDV for 2 hours at 4° C. Mixtures were adsorbed onto BHK-21 or VeroE6 cells in a 96-well plate for 1 hour at 37° C. After washing, cells were incubated for 24 hours and the number of ANDV infected cells was quantitated by immunoperoxidase staining of the nucleocapsid protein as previously described (86). Results were reproduced in at least two separate experiments and presented as a percent of mock treated controls.

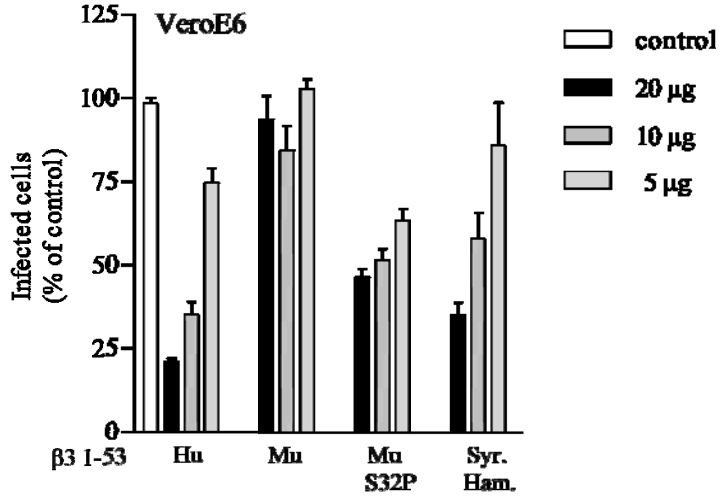

Figure 19 Murine β_3 Integrin PSI Domain Mutants Inhibit ANDV Infection. Increasing amounts (5-20 µg) of human (Hu), murine (Mu), murine S32P (Mu S32P)and Syrian hamster (Syr. Ham.) β_3 integrin PSI domains were incubated with ~1000 FFUs of ANDV for 2 hours at 4° C. Mixtures were adsorbed to VeroE6 cells in a 96-well plate for 1 hour at 37° C. After washing, cells were incubated for 24 hours and the number of ANDV infected cells was quantitated by immunoperoxidase staining of the nucleocapsid protein as previously described (86). Results were reproduced in at least two separate experiments and presented as a percent of mock treated controls.

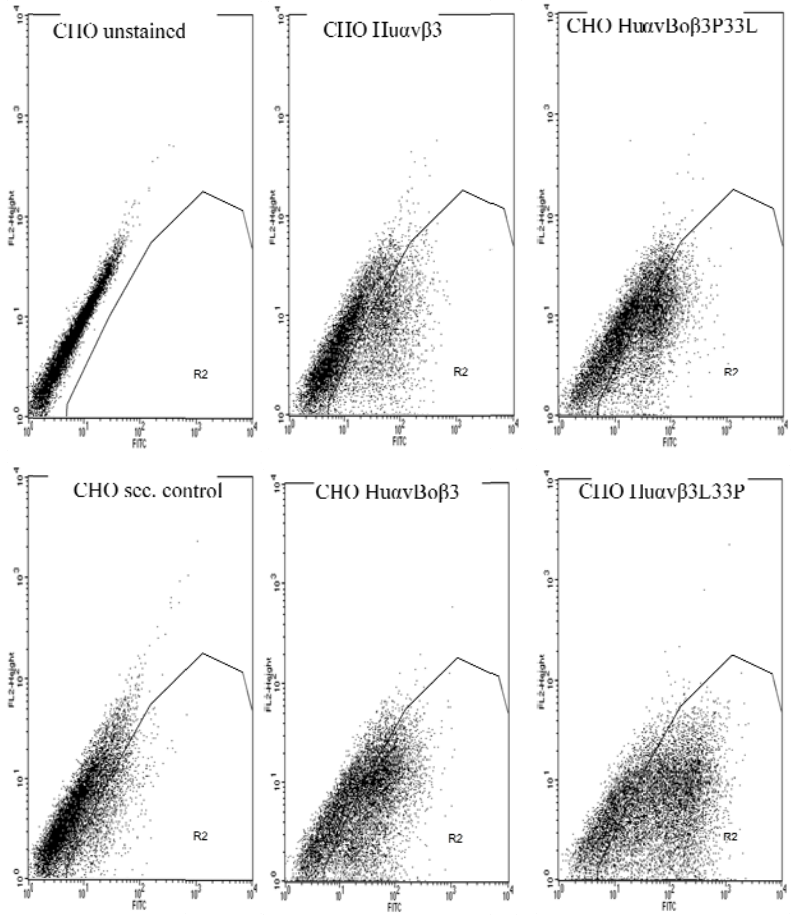

Figure 20 Frequency Histograms representing Expression of $\alpha_v\beta_3$ Integrins on Cell surface of CHO cells.CHO cells were transfected with equal amounts of human α_v and either human β_3 , human mutants, bovine or bovine mutants β_3 expression plasmids. Two days post-transfection, dissociated cells were incubated with anti- $\alpha_v\beta_3$ integrin (LM609) followed by incubation with anti-mouse FITC and cell surface expression was analyzed by flow cytometry. Regions R1 and R2 were set according to fluorescence (FITC).

		Events	% Gated	% Total	Mean	Geo Mean	Median
CHO FITC	**All**	**10,000**	**100**	**99.96**	**14.09**	**8.01**	**7.14**
	M1	**8004**	**80.04**	**80.01**	**6.86**	**5.52**	**5.52**
	M2	**2011**	**20.11**	**20.1**	**42.87**	**35.5**	**32.2**
CHO Hu αvβ3	**All**	**10,000**	**100**	**99.97**	**29.72**	**13.35**	**11.24**
	M1	**6490**	**64.9**	**64.88**	**7.67**	**6.36**	**6.61**
	M2	**3527**	**35.27**	**35.26**	**70.25**	**52.33**	**47.83**
CHO Huαv Boβ3	**All**	**10,000**	**100**	**99.91**	**44.16**	**22.05**	**22.88**
	M1	**4490**	**44.9**	**44.86**	**8.82**	**7.26**	**8.13**
	M2	**5534**	**55.34**	**55.29**	**72.72**	**54.25**	**49.58**
CHO HuαvBoβ3P33L	**All**	**10,000**	**100**	**99.91**	**36.03**	**19.3**	**19.81**
	M1	**4898**	**48.98**	**48.94**	**8.85**	**7.26**	**8.28**
	M2	**5132**	**51.32**	**51.27**	**61.88**	**49.09**	**46.56**
CHO Huαvβ3L33P	**All**	**10,000**	**100**	**99.94**	**132.5**	**47.18**	**53.28**
	M1	**3145**	**31.45**	**31.43**	**8.89**	**7.52**	**8.2**
	M2	**6866**	**68.66**	**68.62**	**175.83**	**109.23**	**110.4**

Table 2 Levels of recombinant β3 integrins expressed on the surface of transfected CHO cells. CHO cells were transfected with equal amounts of human α_v and either human β_3, human mutants, bovine or bovine mutants β_3 expression plasmids. Two days post-transfection, dissociated cells were incubated with anti- $\alpha_v\beta_3$ integrin (LM609) followed by incubation with anti-mouse FITC and cell surface expression was analyzed by flow cytometry. M1 and M2 are two distinct populations set according to fluorescence (FITC). The numbers reported are the total events (stained and unstained) measured, % total (unstained and stained) events, % events within the unstained and stained evetns, mean of stained and unstained events (linear scale), Geometric mean of stained and unstained events (log scale) and median of stained and unstained events.

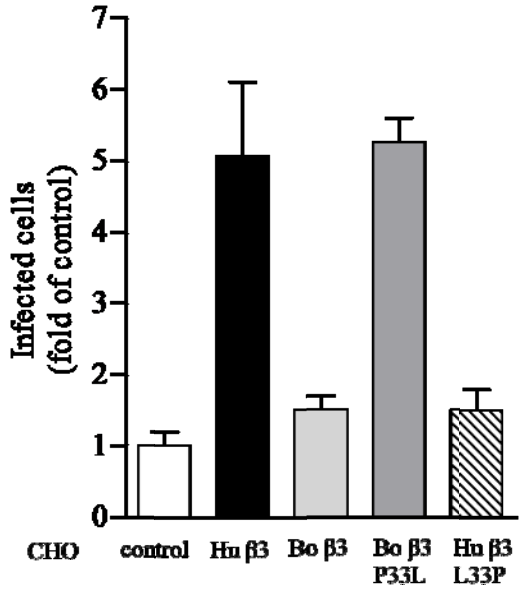

Figure 21 Bovine β_3 Integrin P33L Confers Cell Susceptibility to ANDV Infection. CHO cells were co-transfected with recombinant human αv integrin subunits along with human wild type β_3, bovine wild type β_3, mutant bovine P33L β_3 or human L33P β_3 integrin subunits. Cell surface expression of $\alpha_v\beta_3$ integrins was determined by flow cytometry and cells were subsequently infected with ~1000 FFU of ANDV for one hour at 37° C. Following viral adsorption, inocula were removed and cells were washed and incubated 24 hours at 37° C before fixation. Infected CHO cells were quantitated by immunoperoxidase staining of the nucleocapsid protein as previously described (86). Results were reproduced in at least two separate experiments and presented as fold of mock transfected controls.

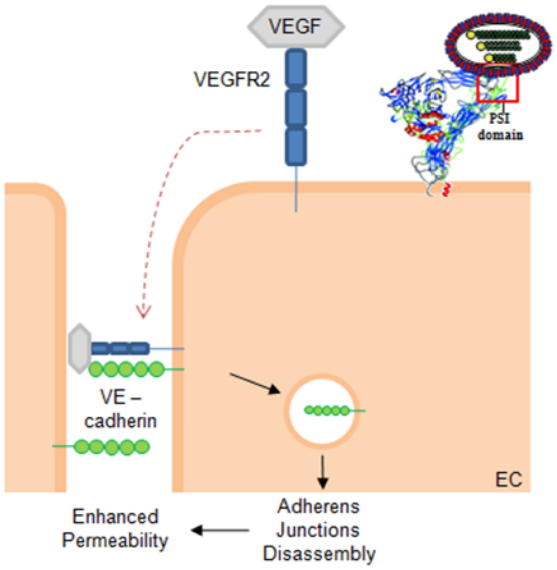

Figure 22 Proposed model for hantavirus regulation of vascular permeability. VEGF binding to VEGFR2 regulates the internalization of the adherens junction protein VE-cadherin and leads to the disassembly of endothelial cell junctions. Pathogenic hantaviruses keep the αvβ3 integrin in an inactive state. Inactive αvβ3 integrins may be unable to regulate VEGFR2 which may lead to an increased internalization of VE-cadherin and an enhanced permeability.

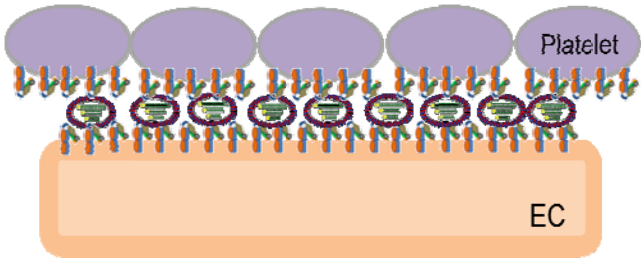

Figure 23 Potential model of Platelet Recruitment by Pathogenic hantavirus infected Cells. Cell associated hantaviruses on the surface of infected endothelial cells may direct the recruitment of platelets to the endothelium via inactive bent β3 integrins present on the surface of platelets and endothelial cells.

References

1. **Aleksandrowicz, P., K. Wolf, D. Falzarano, H. Feldmann, J. Seebach, and H. Schnittler.** 2008. Viral haemorrhagic fever and vascular alterations. Hamostaseologie **28:**77-84.
2. **Alff, P. J., I. N. Gavrilovskaya, E. Gorbunova, K. Endriss, Y. Chong, E. Geimonen, N. Sen, N. C. Reich, and E. R. Mackow.** 2006. The pathogenic NY-1 hantavirus G1 cytoplasmic tail inhibits RIG-I- and TBK-1-directed interferon responses. J Virol **80:**9676-86.
3. **Alff, P. J., N. Sen, E. Gorbunova, I. N. Gavrilovskaya, and E. R. Mackow.** 2008. The NY-1 hantavirus Gn cytoplasmic tail coprecipitates TRAF3 and inhibits cellular interferon responses by disrupting TBK1-TRAF3 complex formation. J Virol **82:**9115-22.
4. **Altmeyer, R.** 2004. Virus attachment and entry offer numerous targets for antiviral therapy. Curr Pharm Des **10:**3701-12.
5. **Arnaout, M. A.** 2002. Integrin structure: new twists and turns in dynamic cell adhesion. Immunol Rev **186:**125-40.
6. **Aster, R. H.** 2005. Immune thrombocytopenia caused by glycoprotein IIb/IIIa inhibitors. Chest **127:**53S-59S.
7. **Basu, A., and U. C. Chaturvedi.** 2008. Vascular endothelium: the battlefield of dengue viruses. FEMS Immunol Med Microbiol **53:**287-99.
8. **Bernshtein, A. D., N. S. Apekina, T. V. Mikhailova, Y. A. Myasnikov, L. A. Khlyap, Y. S. Korotkov, and I. N. Gavrilovskaya.** 1999. Dynamics of Puumala hantavirus infection in naturally infected bank voles (Clethrinomys glareolus). Arch Virol **144:**2415-28.
9. **Brakenhielm, E.** 2007. Substrate matters: reciprocally stimulatory integrin and VEGF signaling in endothelial cells. Circ Res **101:**536-8.
10. **Burgess, J. K.** 2001. Molecular mechanisms of drug-induced thrombocytopenia. Curr Opin Hematol **8:**294-8.
11. **Byzova, T. V., C. K. Goldman, N. Pampori, K. A. Thomas, A. Bett, S. J. Shattil, and E. F. Plow.** 2000. A mechanism for modulation of cellular responses to VEGF: activation of the integrins. Mol Cell **6:**851-60.
12. **Byzova, T. V., R. Rabbani, S. E. D'Souza, and E. F. Plow.** 1998. Role of integrin alpha(v)beta3 in vascular biology. Thromb Haemost **80:**726-34.
13. **Chen, J. P., and T. M. Cosgriff.** 2000. Hemorrhagic fever virus-induced changes in hemostasis and vascular biology. Blood Coagul Fibrinolysis **11:**461-83.
14. **Cines, D. B., E. S. Pollak, C. A. Buck, J. Loscalzo, G. A. Zimmerman, R. P. McEver, J. S. Pober, T. M. Wick, B. A. Konkle, B. S. Schwartz, E. S. Barnathan, K. R. McCrae, B. A. Hug, A. M. Schmidt, and D. M. Stern.** 1998. Endothelial cells in physiology and in the pathophysiology of vascular disorders. Blood **91:**3527-61.
15. **Clement, J. P.** 2003. Hantavirus. Antiviral Res **57:**121-7.
16. **Coller, B. S., and S. J. Shattil.** 2008. The GPIIb/IIIa (integrin alphaIIbbeta3) odyssey: a technology-driven saga of a receptor with twists, turns, and even a bend. Blood **112:**3011-25.
17. **Cosgriff, T. M.** 1991. Mechanisms of disease in Hantavirus infection: pathophysiology of hemorrhagic fever with renal syndrome. Rev Infect Dis **13:**97-107.
18. **Cosgriff, T. M., and R. M. Lewis.** 1991. Mechanisms of disease in hemorrhagic fever with renal syndrome. Kidney Int Suppl **35:**S72-9.

19. **Custer, D. M., E. Thompson, C. S. Schmaljohn, T. G. Ksiazek, and J. W. Hooper.** 2003. Active and passive vaccination against hantavirus pulmonary syndrome with Andes virus M genome segment-based DNA vaccine. J Virol **77:**9894-905.
20. **Doms, R. W.** 2004. Viral entry denied. N Engl J Med **351:**743-4.
21. **Enria, D., P. Padula, E. L. Segura, N. Pini, A. Edelstein, C. R. Posse, and M. C. Weissenbacher.** 1996. Hantavirus pulmonary syndrome in Argentina. Possibility of person to person transmission. Medicina (B Aires) **56:**709-11.
22. **Farmer, C., P. E. Morton, M. Snippe, G. Santis, and M. Parsons.** 2009. Coxsackie adenovirus receptor (CAR) regulates integrin function through activation of p44/42 MAPK. Exp Cell Res.
23. **Galeno, H., J. Mora, E. Villagra, J. Fernandez, J. Hernandez, G. J. Mertz, and E. Ramirez.** 2002. First human isolate of Hantavirus (Andes virus) in the Americas. Emerg Infect Dis **8:**657-61.
24. **Gavard, J., and J. S. Gutkind.** 2006. VEGF controls endothelial-cell permeability by promoting the beta-arrestin-dependent endocytosis of VE-cadherin. Nat Cell Biol **8:**1223-34.
25. **Gavard, J., V. Patel, and J. S. Gutkind.** 2008. Angiopoietin-1 prevents VEGF-induced endothelial permeability by sequestering Src through mDia. Dev Cell **14:**25-36.
26. **Gavrilovskaya, I. N., E. J. Brown, M. H. Ginsberg, and E. R. Mackow.** 1999. Cellular entry of hantaviruses which cause hemorrhagic fever with renal syndrome is mediated by beta3 integrins. J Virol **73:**3951-9.
27. **Gavrilovskaya, I. N., E. E. Gorbunova, N. A. Mackow, and E. R. Mackow.** 2008. Hantaviruses direct endothelial cell permeability by sensitizing cells to the vascular permeability factor VEGF, while angiopoietin 1 and sphingosine 1-phosphate inhibit hantavirus-directed permeability. J Virol **82:**5797-806.
28. **Gavrilovskaya, I. N., T. Peresleni, E. Geimonen, and E. R. Mackow.** 2002. Pathogenic hantaviruses selectively inhibit beta3 integrin directed endothelial cell migration. Arch Virol **147:**1913-31.
29. **Gavrilovskaya, I. N., M. Shepley, R. Shaw, M. H. Ginsberg, and E. R. Mackow.** 1998. beta3 Integrins mediate the cellular entry of hantaviruses that cause respiratory failure. Proc Natl Acad Sci U S A **95:**7074-9.
30. **Geimonen, E., I. Fernandez, I. N. Gavrilovskaya, and E. R. Mackow.** 2003. Tyrosine residues direct the ubiquitination and degradation of the NY-1 hantavirus G1 cytoplasmic tail. J Virol **77:**10760-868.
31. **Geimonen, E., R. LaMonica, K. Springer, Y. Farooqui, I. N. Gavrilovskaya, and E. R. Mackow.** 2003. Hantavirus pulmonary syndrome-associated hantaviruses contain conserved and functional ITAM signaling elements. J Virol **77:**1638-43.
32. **Geimonen, E., S. Neff, T. Raymond, S. S. Kocer, I. N. Gavrilovskaya, and E. R. Mackow.** 2002. Pathogenic and nonpathogenic hantaviruses differentially regulate endothelial cell responses. Proc Natl Acad Sci U S A **99:**13837-42.
33. **Ginsberg, M. H., A. Partridge, and S. J. Shattil.** 2005. Integrin regulation. Curr Opin Cell Biol **17:**509-16.
34. **Goldsmith, C. S., L. H. Elliott, C. J. Peters, and S. R. Zaki.** 1995. Ultrastructural characteristics of Sin Nombre virus, causative agent of hantavirus pulmonary syndrome. Arch Virol **140:**2107-22.
35. **Hall, P. R., B. Hjelle, H. Njus, C. Ye, V. Bondu-Hawkins, D. C. Brown, K. A. Kilpatrick, and R. S. Larson.** 2009. Phage-display selection of cyclic peptides which inhibit Andes virus infection. J Virol.

36. **Hall, P. R., L. Malone, L. O. Sillerud, C. Ye, B. L. Hjelle, and R. S. Larson.** 2007. Characterization and NMR solution structure of a novel cyclic pentapeptide inhibitor of pathogenic hantaviruses. Chem Biol Drug Des **69:**180-90.
37. **Harris, K., P. Nguyen, and E. M. Van Cott.** 2008. Platelet PlA2 Polymorphism and the risk for thrombosis in heparin-induced thrombocytopenia. Am J Clin Pathol **129:**282-6.
38. **Hayasaka, D., K. Maeda, F. A. Ennis, and M. Terajima.** 2007. Increased permeability of human endothelial cell line EA.hy926 induced by hantavirus-specific cytotoxic T lymphocytes. Virus Res **123:**120-7.
39. **Hippenstiel, S., and N. Suttorp.** 2003. Interaction of pathogens with the endothelium. Thromb Haemost **89:**18-24.
40. **Hjelle, B., and T. Yates.** 2001. Modeling hantavirus maintenance and transmission in rodent communities. Curr Top Microbiol Immunol **256:**77-90.
41. **Hodivala-Dilke, K. M., K. P. McHugh, D. A. Tsakiris, H. Rayburn, D. Crowley, M. Ullman-Cullere, F. P. Ross, B. S. Coller, S. Teitelbaum, and R. O. Hynes.** 1999. Beta3-integrin-deficient mice are a model for Glanzmann thrombasthenia showing placental defects and reduced survival. J Clin Invest **103:**229-38.
42. **Hood, J. D., and D. A. Cheresh.** 2002. Role of integrins in cell invasion and migration. Nat Rev Cancer **2:**91-100.
43. **Hooper, J. W., A. M. Ferro, and V. Wahl-Jensen.** 2008. Immune serum produced by DNA vaccination protects hamsters against lethal respiratory challenge with Andes virus. J Virol **82:**1332-8.
44. **Hooper, J. W., T. Larsen, D. M. Custer, and C. S. Schmaljohn.** 2001. A lethal disease model for hantavirus pulmonary syndrome. Virology **289:**6-14.
45. **Humphries, M. J., P. A. McEwan, S. J. Barton, P. A. Buckley, J. Bella, and A. P. Mould.** 2003. Integrin structure: heady advances in ligand binding, but activation still makes the knees wobble. Trends Biochem Sci **28:**313-20.
46. **Hynes, R. O.** 2002. Integrins: bidirectional, allosteric signaling machines. Cell **110:**673-87.
47. **Johnson, K. M.** 2001. Hantaviruses: history and overview. Curr Top Microbiol Immunol **256:**1-14.
48. **Jonsson, C. B., and C. S. Schmaljohn.** 2001. Replication of hantaviruses. Curr Top Microbiol Immunol **256:**15-32.
49. **Joutsi-Korhonen, L., S. Preston, P. A. Smethurst, M. Ijsseldijk, E. Schaffner-Reckinger, K. L. Armour, N. A. Watkins, M. R. Clark, P. G. de Groot, R. W. Farndale, W. H. Ouwehand, and L. M. Williamson.** 2004. The effect of recombinant IgG antibodies against the leucine-33 form of the platelet beta3 integrin (HPA-1a) on platelet function. Thromb Haemost **91:**743-54.
50. **Kaplan, C.** 2002. Alloimmune thrombocytopenia of the fetus and the newborn. Blood Rev **16:**69-72.
51. **Kaplan, C.** 2002. Platelet alloimmunity: the fetal/neonatal alloimmune thrombocytopenia. Vox Sang **83 Suppl 1:**289-91.
52. **Kaushik-Basu, N., A. Basu, and D. Harris.** 2008. Peptide inhibition of HIV-1: current status and future potential. BioDrugs **22:**161-75.
53. **Khaiboullina, S. F., D. M. Netski, P. Krumpe, and S. C. St Jeor.** 2000. Effects of tumor necrosis factor alpha on sin nombre virus infection in vitro. J Virol **74:**11966-71.
54. **Kilpatrick, E. D., M. Terajima, F. T. Koster, M. D. Catalina, J. Cruz, and F. A. Ennis.** 2004. Role of specific CD8+ T cells in the severity of a fulminant zoonotic viral hemorrhagic fever, hantavirus pulmonary syndrome. J Immunol **172:**3297-304.

55. **Krakauer, T., J. W. Leduc, J. C. Morrill, A. O. Anderson, and H. Krakauer.** 1994. Serum levels of alpha and gamma interferons in hemorrhagic fever with renal syndrome. Viral Immunol **7:**97-101.
56. **Lampugnani, M. G., and E. Dejana.** 2007. The control of endothelial cell functions by adherens junctions. Novartis Found Symp **283:**4-13; discussion 13-7, 238-41.
57. **Lampugnani, M. G., A. Zanetti, F. Breviario, G. Balconi, F. Orsenigo, M. Corada, R. Spagnuolo, M. Betson, V. Braga, and E. Dejana.** 2002. VE-cadherin regulates endothelial actin activating Rac and increasing membrane association of Tiam. Mol Biol Cell **13:**1175-89.
58. **Larson, R. S., D. C. Brown, C. Ye, and B. Hjelle.** 2005. Peptide antagonists that inhibit Sin Nombre virus and hantaan virus entry through the beta3-integrin receptor. J Virol **79:**7319-26.
59. **Lee, A. M., J. M. Rojek, C. F. Spiropoulou, A. T. Gundersen, W. Jin, A. Shaginian, J. York, J. H. Nunberg, D. L. Boger, M. B. Oldstone, and S. Kunz.** 2008. Unique small molecule entry inhibitors of hemorrhagic fever arenaviruses. J Biol Chem **283:**18734-42.
60. **Lee, H. W.** 1989. Hemorrhagic fever with renal syndrome in Korea. Rev Infect Dis **11 Suppl 4:**S864-76.
61. **Lee, H. W., and G. van der Groen.** 1989. Hemorrhagic fever with renal syndrome. Prog Med Virol **36:**62-102.
62. **Linderholm, M., C. Ahlm, B. Settergren, A. Waage, and A. Tarnvik.** 1996. Elevated plasma levels of tumor necrosis factor (TNF)-alpha, soluble TNF receptors, interleukin (IL)-6, and IL-10 in patients with hemorrhagic fever with renal syndrome. J Infect Dis **173:**38-43.
63. **Liu, Z., M. Gao, Q. Han, S. Lou, and J. Fang.** 2009. Platelet glycoprotein IIb/IIIa (HPA-1 and HPA-3) polymorphisms in patients with hemorrhagic fever with renal syndrome. Hum Immunol **70:**452-6.
64. **Lober, C., B. Anheier, S. Lindow, H. D. Klenk, and H. Feldmann.** 2001. The Hantaan virus glycoprotein precursor is cleaved at the conserved pentapeptide WAASA. Virology **289:**224-9.
65. **Loncar, R., V. Stoldt, S. Hellmig, R. B. Zotz, M. Mihalj, and R. E. Scharf.** 2007. HPA-1 polymorphism of alphaIIbbeta3 modulates platelet adhesion onto immobilized fibrinogen in an in-vitro flow system. Thromb J **5:**2.
66. **Lundkvist, A., V. Vasilenko, I. Golovljova, A. Plyusnin, and A. Vaheri.** 1998. Human Dobrava hantavirus infections in Estonia. Lancet **352:**369.
67. **Luo, B. H., C. V. Carman, and T. A. Springer.** 2007. Structural basis of integrin regulation and signaling. Annu Rev Immunol **25:**619-47.
68. **Mackow, E. R., and I. N. Gavrilovskaya.** 2001. Cellular receptors and hantavirus pathogenesis. Curr Top Microbiol Immunol **256:**91-115.
69. **Maes, P., J. Clement, I. Gavrilovskaya, and M. Van Ranst.** 2004. Hantaviruses: immunology, treatment, and prevention. Viral Immunol **17:**481-97.
70. **Maes, P., J. Clement, P. H. Groeneveld, P. Colson, T. W. Huizinga, and M. Van Ranst.** 2006. Tumor necrosis factor-alpha genetic predisposing factors can influence clinical severity in nephropathia epidemica. Viral Immunol **19:**558-64.
71. **Mir, M. A., W. A. Duran, B. L. Hjelle, C. Ye, and A. T. Panganiban.** 2008. Storage of cellular 5' mRNA caps in P bodies for viral cap-snatching. Proc Natl Acad Sci U S A **105:**19294-9.
72. **Mori, M., A. L. Rothman, I. Kurane, J. M. Montoya, K. B. Nolte, J. E. Norman, D. C. Waite, F. T. Koster, and F. A. Ennis.** 1999. High levels of cytokine-producing cells

in the lung tissues of patients with fatal hantavirus pulmonary syndrome. J Infect Dis **179:**295-302.

73. **Neff, S., and B. Baxt.** 2001. The ability of integrin alpha(v)beta(3) To function as a receptor for foot-and-mouth disease virus is not dependent on the presence of complete subunit cytoplasmic domains. J Virol **75:**527-32.
74. **Nerurkar, V. R., J. W. Song, K. J. Song, J. W. Nagle, B. Hjelle, S. Jenison, and R. Yanagihara.** 1994. Genetic evidence for a hantavirus enzootic in deer mice (Peromyscus maniculatus) captured a decade before the recognition of hantavirus pulmonary syndrome. Virology **204:**563-8.
75. **Niikura, M., A. Maeda, T. Ikegami, M. Saijo, I. Kurane, and S. Morikawa.** 2004. Modification of endothelial cell functions by Hantaan virus infection: prolonged hyper-permeability induced by TNF-alpha of hantaan virus-infected endothelial cell monolayers. Arch Virol **149:**1279-92.
76. **Nolte, K. B., R. M. Feddersen, K. Foucar, S. R. Zaki, F. T. Koster, D. Madar, T. L. Merlin, P. J. McFeeley, E. T. Umland, and R. E. Zumwalt.** 1995. Hantavirus pulmonary syndrome in the United States: a pathological description of a disease caused by a new agent. Hum Pathol **26:**110-20.
77. **Olsson, A. K., A. Dimberg, J. Kreuger, and L. Claesson-Welsh.** 2006. VEGF receptor signalling - in control of vascular function. Nat Rev Mol Cell Biol **7:**359-71.
78. **Overby, A. K., V. L. Popov, R. F. Pettersson, and E. P. Neve.** 2007. The cytoplasmic tails of Uukuniemi Virus (Bunyaviridae) G(N) and G(C) glycoproteins are important for intracellular targeting and the budding of virus-like particles. J Virol **81:**11381-91.
79. **Padula, P. J., A. Edelstein, S. D. Miguel, N. M. Lopez, C. M. Rossi, and R. D. Rabinovich.** 1998. Hantavirus pulmonary syndrome outbreak in Argentina: molecular evidence for person-to-person transmission of Andes virus. Virology **241:**323-30.
80. **Peters, C. J., and A. S. Khan.** 2002. Hantavirus pulmonary syndrome: the new American hemorrhagic fever. Clin Infect Dis **34:**1224-31.
81. **Peters, C. J., G. L. Simpson, and H. Levy.** 1999. Spectrum of hantavirus infection: hemorrhagic fever with renal syndrome and hantavirus pulmonary syndrome. Annu Rev Med **50:**531-45.
82. **Peters, C. J., and S. R. Zaki.** 2002. Role of the endothelium in viral hemorrhagic fevers. Crit Care Med **30:**S268-73.
83. **Peterson, J. A., C. E. Nyree, P. J. Newman, and R. H. Aster.** 2003. A site involving the "hybrid" and PSI homology domains of GPIIIa (beta 3-integrin subunit) is a common target for antibodies associated with quinine-induced immune thrombocytopenia. Blood **101:**937-42.
84. **Plyusnin, A., and S. P. Morzunov.** 2001. Virus evolution and genetic diversity of hantaviruses and their rodent hosts. Curr Top Microbiol Immunol **256:**47-75.
85. **Plyusnin, A., O. Vapalahti, and A. Vaheri.** 1996. Hantaviruses: genome structure, expression and evolution. J Gen Virol **77 (Pt 11):**2677-87.
86. **Raymond, T., E. Gorbunova, I. N. Gavrilovskaya, and E. R. Mackow.** 2005. Pathogenic hantaviruses bind plexin-semaphorin-integrin domains present at the apex of inactive, bent alphavbeta3 integrin conformers. Proc Natl Acad Sci U S A **102:**1163-8.
87. **Reynolds, A. R., L. E. Reynolds, T. E. Nagel, J. C. Lively, S. D. Robinson, D. J. Hicklin, S. C. Bodary, and K. M. Hodivala-Dilke.** 2004. Elevated Flk1 (vascular endothelial growth factor receptor 2) signaling mediates enhanced angiogenesis in beta3-integrin-deficient mice. Cancer Res **64:**8643-50.
88. **Reynolds, L. E., L. Wyder, J. C. Lively, D. Taverna, S. D. Robinson, X. Huang, D. Sheppard, R. O. Hynes, and K. M. Hodivala-Dilke.** 2002. Enhanced pathological

angiogenesis in mice lacking beta3 integrin or beta3 and beta5 integrins. Nat Med **8:**27-34.

89. **Robinson, S. D., L. E. Reynolds, L. Wyder, D. J. Hicklin, and K. M. Hodivala-Dilke.** 2004. Beta3-integrin regulates vascular endothelial growth factor-A-dependent permeability. Arterioscler Thromb Vasc Biol **24:**2108-14.
90. **Rojek, J. M., and S. Kunz.** 2008. Cell entry by human pathogenic arenaviruses. Cell Microbiol **10:**828-35.
91. **Ruiz, C., C. Y. Liu, Q. H. Sun, M. Sigaud-Fiks, E. Fressinaud, J. Y. Muller, P. Nurden, A. T. Nurden, P. J. Newman, and N. Valentin.** 2001. A point mutation in the cysteine-rich domain of glycoprotein (GP) IIIa results in the expression of a GPIIb-IIIa (alphaIIbbeta3) integrin receptor locked in a high-affinity state and a Glanzmann thrombasthenia-like phenotype. Blood **98:**2432-41.
92. **Schaffner-Reckinger, E.** 2003. Beta3 integrins: major therapeutic targets of the near future. Bull Soc Sci Med Grand Duche Luxemb**:**23-34.
93. **Schaphorst, K. L., E. Chiang, K. N. Jacobs, A. Zaiman, V. Natarajan, F. Wigley, and J. G. Garcia.** 2003. Role of sphingosine-1 phosphate in the enhancement of endothelial barrier integrity by platelet-released products. Am J Physiol Lung Cell Mol Physiol **285:**L258-67.
94. **Schmaljohn, C., and B. Hjelle.** 1997. Hantaviruses: a global disease problem. Emerg Infect Dis **3:**95-104.
95. **Schonrich, G., A. Rang, N. Lutteke, M. J. Raftery, N. Charbonnel, and R. G. Ulrich.** 2008. Hantavirus-induced immunity in rodent reservoirs and humans. Immunol Rev **225:**163-89.
96. **Sen, N., A. Sen, and E. R. Mackow.** 2007. Degrons at the C terminus of the pathogenic but not the nonpathogenic hantavirus G1 tail direct proteasomal degradation. J Virol **81:**4323-30.
97. **Shi, M., K. Sundramurthy, B. Liu, S. M. Tan, S. K. Law, and J. Lescar.** 2005. The crystal structure of the plexin-semaphorin-integrin domain/hybrid domain/I-EGF1 segment from the human integrin beta2 subunit at 1.8-A resolution. J Biol Chem **280:**30586-93.
98. **Shi, X., and R. M. Elliott.** 2002. Golgi localization of Hantaan virus glycoproteins requires coexpression of G1 and G2. Virology **300:**31-8.
99. **Soldi, R., S. Mitola, M. Strasly, P. Defilippi, G. Tarone, and F. Bussolino.** 1999. Role of alphavbeta3 integrin in the activation of vascular endothelial growth factor receptor-2. EMBO J **18:**882-92.
100. **Spiropoulou, C. F.** 2001. Hantavirus maturation. Curr Top Microbiol Immunol **256:**33-46.
101. **Stenmark, K. R., K. A. Fagan, and M. G. Frid.** 2006. Hypoxia-induced pulmonary vascular remodeling: cellular and molecular mechanisms. Circ Res **99:**675-91.
102. **Stewart, P. L., and G. R. Nemerow.** 2007. Cell integrins: commonly used receptors for diverse viral pathogens. Trends Microbiol **15:**500-7.
103. **Sun, G. D., X. M. Duan, Y. P. Zhang, Z. Z. Yin, X. L. Niu, Y. F. Li, H. J. Niu, and Y. L. Zhao.** 2005. [Analysis of genetic polymorphism in randomized donor's HPA 1-16 antigens and establishment of typed platelet donor data bank]. Zhongguo Shi Yan Xue Ye Xue Za Zhi **13:**889-95.
104. **Sundstrom, J. B., L. K. McMullan, C. F. Spiropoulou, W. C. Hooper, A. A. Ansari, C. J. Peters, and P. E. Rollin.** 2001. Hantavirus infection induces the expression of RANTES and IP-10 without causing increased permeability in human lung microvascular endothelial cells. J Virol **75:**6070-85.

105. **Takagi, J., B. M. Petre, T. Walz, and T. A. Springer.** 2002. Global conformational rearrangements in integrin extracellular domains in outside-in and inside-out signaling. Cell **110:**599-11.
106. **Tang, N., L. Wang, J. Esko, F. J. Giordano, Y. Huang, H. P. Gerber, N. Ferrara, and R. S. Johnson.** 2004. Loss of HIF-1alpha in endothelial cells disrupts a hypoxia-driven VEGF autocrine loop necessary for tumorigenesis. Cancer Cell **6:**485-95.
107. **Tani, M., T. Sano, M. Ito, and Y. Igarashi.** 2005. Mechanisms of sphingosine and sphingosine 1-phosphate generation in human platelets. J Lipid Res **46:**2458-67.
108. **Taylor, S. L., N. Frias-Staheli, A. Garcia-Sastre, and C. S. Schmaljohn.** 2009. Hantaan virus nucleocapsid protein binds to importin alpha proteins and inhibits tumor necrosis factor alpha-induced activation of nuclear factor kappa B. J Virol **83:**1271-9.
109. **Temonen, M., J. Mustonen, H. Helin, A. Pasternack, A. Vaheri, and H. Holthofer.** 1996. Cytokines, adhesion molecules, and cellular infiltration in nephropathia epidemica kidneys: an immunohistochemical study. Clin Immunol Immunopathol **78:**47-55.
110. **Terajima, M., J. D. Hendershot, 3rd, H. Kariwa, F. T. Koster, B. Hjelle, D. Goade, M. C. DeFronzo, and F. A. Ennis.** 1999. High levels of viremia in patients with the Hantavirus pulmonary syndrome. J Infect Dis **180:**2030-4.
111. **Thurston, G., J. S. Rudge, E. Ioffe, H. Zhou, L. Ross, S. D. Croll, N. Glazer, J. Holash, D. M. McDonald, and G. D. Yancopoulos.** 2000. Angiopoietin-1 protects the adult vasculature against plasma leakage. Nat Med **6:**460-3.
112. **Thurston, G., C. Suri, K. Smith, J. McClain, T. N. Sato, G. D. Yancopoulos, and D. M. McDonald.** 1999. Leakage-resistant blood vessels in mice transgenically overexpressing angiopoietin-1. Science **286:**2511-4.
113. **Toro, J., J. D. Vega, A. S. Khan, J. N. Mills, P. Padula, W. Terry, Z. Yadon, R. Valderrama, B. A. Ellis, C. Pavletic, R. Cerda, S. Zaki, W. J. Shieh, R. Meyer, M. Tapia, C. Mansilla, M. Baro, J. A. Vergara, M. Concha, G. Calderon, D. Enria, C. J. Peters, and T. G. Ksiazek.** 1998. An outbreak of hantavirus pulmonary syndrome, Chile, 1997. Emerg Infect Dis **4:**687-94.
114. **Tuvim, M. J., S. E. Evans, C. G. Clement, B. F. Dickey, and B. E. Gilbert.** 2009. Augmented lung inflammation protects against influenza A pneumonia. PLoS One **4:**e4176.
115. **Undas, A., K. Brummel, J. Musial, K. G. Mann, and A. Szczeklik.** 2001. Pl(A2) polymorphism of beta(3) integrins is associated with enhanced thrombin generation and impaired antithrombotic action of aspirin at the site of microvascular injury. Circulation **104:**2666-72.
116. **Valbuena, G., and D. H. Walker.** 2006. The endothelium as a target for infections. Annu Rev Pathol **1:**171-98.
117. **van Gils, J. M., J. Stutterheim, T. J. van Duijn, J. J. Zwaginga, L. Porcelijn, M. de Haas, and P. L. Hordijk.** 2009. HPA-1a alloantibodies reduce endothelial cell spreading and monolayer integrity. Mol Immunol **46:**406-15.
118. **Verheul, H. M., A. S. Jorna, K. Hoekman, H. J. Broxterman, M. F. Gebbink, and H. M. Pinedo.** 2000. Vascular endothelial growth factor-stimulated endothelial cells promote adhesion and activation of platelets. Blood **96:**4216-21.
119. **Vijayan, K. V., and P. F. Bray.** 2006. Molecular mechanisms of prothrombotic risk due to genetic variations in platelet genes: Enhanced outside-in signaling through the Pro33 variant of integrin beta3. Exp Biol Med (Maywood) **231:**505-13.
120. **Vijayan, K. V., P. J. Goldschmidt-Clermont, C. Roos, and P. F. Bray.** 2000. The Pl(A2) polymorphism of integrin beta(3) enhances outside-in signaling and adhesive functions. J Clin Invest **105:**793-802.

121. **Wahl-Jensen, V., J. Chapman, L. Asher, R. Fisher, M. Zimmerman, T. Larsen, and J. W. Hooper.** 2007. Temporal analysis of Andes virus and Sin Nombre virus infections of Syrian hamsters. J Virol **81:**7449-62.
122. **Wallez, Y., I. Vilgrain, and P. Huber.** 2006. Angiogenesis: the VE-cadherin switch. Trends Cardiovasc Med **16:**55-9.
123. **Wang, X., D. Y. Huang, S. M. Huong, and E. S. Huang.** 2005. Integrin alphavbeta3 is a coreceptor for human cytomegalovirus. Nat Med **11:**515-21.
124. **Watkins, N. A., P. A. Smethurst, D. Allen, G. A. Smith, and W. H. Ouwehand.** 2002. Platelet alphaIIbbeta3 recombinant autoantibodies from the B-cell repertoire of a post-transfusion purpura patient. Br J Haematol **116:**677-85.
125. **Weber, F., and A. Mirazimi.** 2008. Interferon and cytokine responses to Crimean Congo hemorrhagic fever virus; an emerging and neglected viral zonoosis. Cytokine Growth Factor Rev **19:**395-404.
126. **Wells, R. M., S. Sosa Estani, Z. E. Yadon, D. Enria, P. Padula, N. Pini, J. N. Mills, C. J. Peters, and E. L. Segura.** 1997. An unusual hantavirus outbreak in southern Argentina: person-to-person transmission? Hantavirus Pulmonary Syndrome Study Group for Patagonia. Emerg Infect Dis **3:**171-4.
127. **Whitehouse, C. A.** 2004. Crimean-Congo hemorrhagic fever. Antiviral Res **64:**145-60.
128. **Wu, M. H.** 2005. Endothelial focal adhesions and barrier function. J Physiol **569:**359-66.
129. **Xiong, J. P., T. Stehle, S. L. Goodman, and M. A. Arnaout.** 2004. A novel adaptation of the integrin PSI domain revealed from its crystal structure. J Biol Chem **279:**40252-4.
130. **Xiong, J. P., T. Stehle, R. Zhang, A. Joachimiak, M. Frech, S. L. Goodman, and M. A. Arnaout.** 2002. Crystal structure of the extracellular segment of integrin alpha Vbeta3 in complex with an Arg-Gly-Asp ligand. Science **296:**151-5.
131. **Zaki, S. R., P. W. Greer, L. M. Coffield, C. S. Goldsmith, K. B. Nolte, K. Foucar, R. M. Feddersen, R. E. Zumwalt, G. L. Miller, A. S. Khan, and et al.** 1995. Hantavirus pulmonary syndrome. Pathogenesis of an emerging infectious disease. Am J Pathol **146:**552-79.
132. **Zanetti, A., M. G. Lampugnani, G. Balconi, F. Breviario, M. Corada, L. Lanfrancone, and E. Dejana.** 2002. Vascular endothelial growth factor induces SHC association with vascular endothelial cadherin: a potential feedback mechanism to control vascular endothelial growth factor receptor-2 signaling. Arterioscler Thromb Vasc Biol **22:**617-22.
133. **Zhu, J., B. Boylan, B. H. Luo, P. J. Newman, and T. A. Springer.** 2007. Tests of the extension and deadbolt models of integrin activation. J Biol Chem **282:**11914-20.